BMT. Recipient rats were given fractionated irradiation (≥4.5 Gy×2) with prior injection of fludarabine, and BMCs (1×10^8) from donor F344 rats were injected intravenously (IV-BMT). In these conditions (1×10^8 BMCs and ≥4.5 Gy×2), macrochimerism (>90%) was established in the recipient rats regardless of IBM-BMT or IV-BMT (Table 1). Therefore, we next carried out BMT with a lower dose of BMCs (3×10^7) and a lower irradiation dose (3.5 Gy×2) to make differences in chimersim clear. PBMNCs were collected from the recipient rats every 2 weeks from the second week until the 24th week after the treatment and stained with donor-specific antirat $RT1^l$ mAb and recipient-specific antirat $RT1^n$ mAb to examine the chimerism.

As shown in Figure 1A, all the recipient rats with fludarabine plus irradiation of either 3.5 Gy×2 or 4.0 Gy×2 showed macrochimerism (>70%) after IBM-BMT. It is noted that approximately 80% of PBMNCs were of donor origin even 180 days after IBM-BMT at the lower irradiation dose (3.5 Gy×2), although the PBMNCs of the recipients treated with fludarabine plus 3.5 Gy×2, followed by IV-BMT, were of host origin (Fig. 1A). This macrochimerism achieved by IBM-BMT was maintained stably even 10 months after transplantation (data not shown). Hematolymphoid cells bearing mature lineage markers were also shown to be of donor origin when the cells in the spleen, PBMNCs, and BM were stained with antibodies against CD45R, CD4, CD8, and CD11b plus donor $RT1^l$ (Table 1 and Supplemental Table 1, available for viewing online only). It is noted that the reconstitution of donor multilineage hematolymphoid cells was similarly observed in the bone marrow of injected and noninjected sites (Supplemental Table 2, available for viewing online only). In contrast, IV-BMT after fludarabine plus 3.5 Gy×2 failed to reconstitute the recipients with donor-derived hematolymphoid cells (Table 1). Only a low level of transient donor chimerism, which lasted only about 1 month, was achieved when the rats were conditioned with fludarabine plus 4.0 Gy×2. Thus, the donor macrochimerism was stably maintained by IBM-BMT, and the low levels of chimerism seen at 2 weeks after IV-BMT (fludarabine plus 4.0 Gy×2) were almost undetectable at 4 weeks. These findings clearly indicate that IBM-BMT facilitated the rapid recovery and reconstitution of donor hematolymphoid cells even with less myelotoxic conditioning regimens (fludarabine plus 3.5 Gy×2) in comparison with conventional IV-BMT.

Survival of Cardiac Allografts

After IBM-BMT, cardiac allografts survived for more than 10 months without any signs of rejection or GvHD in the recipients conditioned with either fludarabine plus 3.5 Gy×2 or fludarabine plus 4.0 Gy×2 (Fig. 1B). In contrast, the cardiac allografts with IV-BMT were rejected within 1 month after BMT in the recipients conditioned with fludarabine plus 3.5 Gy×2 (mean survival time: 22.8±5.4

TABLE 1. Analyses of cell surface antigens on donor-derived cells in the spleen of the recipient rats

Rat	N	BMT	Radiation (Gy)	BMCs ($\times10^7$)	Cell surface antigen (%) Donor-derived CD4[a]	Donor-derived CD8	Donor-derived CD45R	Donor-derived CD11b	Donor-derived cells in chimeric rats (%)
[F344→BN]	5	IV	3.5Gy×2	3	0	0	0	0	0
					9.65±0.60	10.34±0.60	68.34±0.67	10.49±1.23	
[F344→BN]	5	IBM	3.5Gy×2	3	6.45±0.56	15.38±1.21	44.87±1.34	11.54±1.85	73.26±8.54
					10.34±0.25	21.29±0.35	62.78±0.64	16.32±0.76	
[F344→BN]	10	IV	4.0Gy×2	3	0	0.02±0.01	0.07±0.02	0	0.12±0.04
					7.67±0.58	16.66±1.25	62.04±015	8.24±0.47	
[F344→BN]	10	IBM	4.0Gy×2	3	12.21±1.42	12.46±2.43	38.25±1.81	6.88±0.88	81.36±8.86
					14.38±2.05	16.04±0.37	54.45±0.62	11.19±0.54	
[F344→BN]	10	IV	4.5Gy×2	10	10.02±1.25	17.68±2.54	56.56±2.47	9.47±1.57	94.26±7.83
					11.32±0.57	19.54±1.25	66.14±0.61	9.83±1.56	
[F344→BN]	10	IBM	4.5Gy×2	10	11.35±2.01	9.98±1.48	67.81±1.56	12.76±2.04	98.34±2.16
					12.54±0.41	10.82±0.63	68.75±0.83	14.87±0.29	
[F344→BN]	10	IV	5.0Gy×2	10	15.22±2.05	19.84±1.34	52.14±2.06	10.01±1.07	96.27±1.80
					16.11±2.57	22.14±1.72	56.13±1.05	10.04±0.21	
[F344→BN]	10	IBM	5.0Gy×2	10	23.65±1.02	11.22±1.84	52.23±2.63	8.39±0.96	99.26±0.45
					24.21±1.12	11.04±0.56	53.74±0.32	8.73±0.57	
F344	5	–	–	–	–	–	–	–	–
					21.29±0.58	26.13±0.54	59.17±0.71	9.13±0.32	
BN	5	–	–	–	–	–	–	–	–
					26.13±0.60	17.63±0.41	49.29±0.16	10.81±0.27	

The cells from the spleen were prepared from the recipient rats 12 weeks after IBM-BMT or IV-BMT, and stained with donor-specific antirat $RT1^l$ mAb and mAb against mature lineage markers (CD4, CD8, CD45R, and CD11b) to examine the reconstitution of the hematolymphoid system. The cells were analyzed using a FACScan. The results are expressed as the mean±SD of more than five rats.

[a]Donor- and recipient-derived cells.

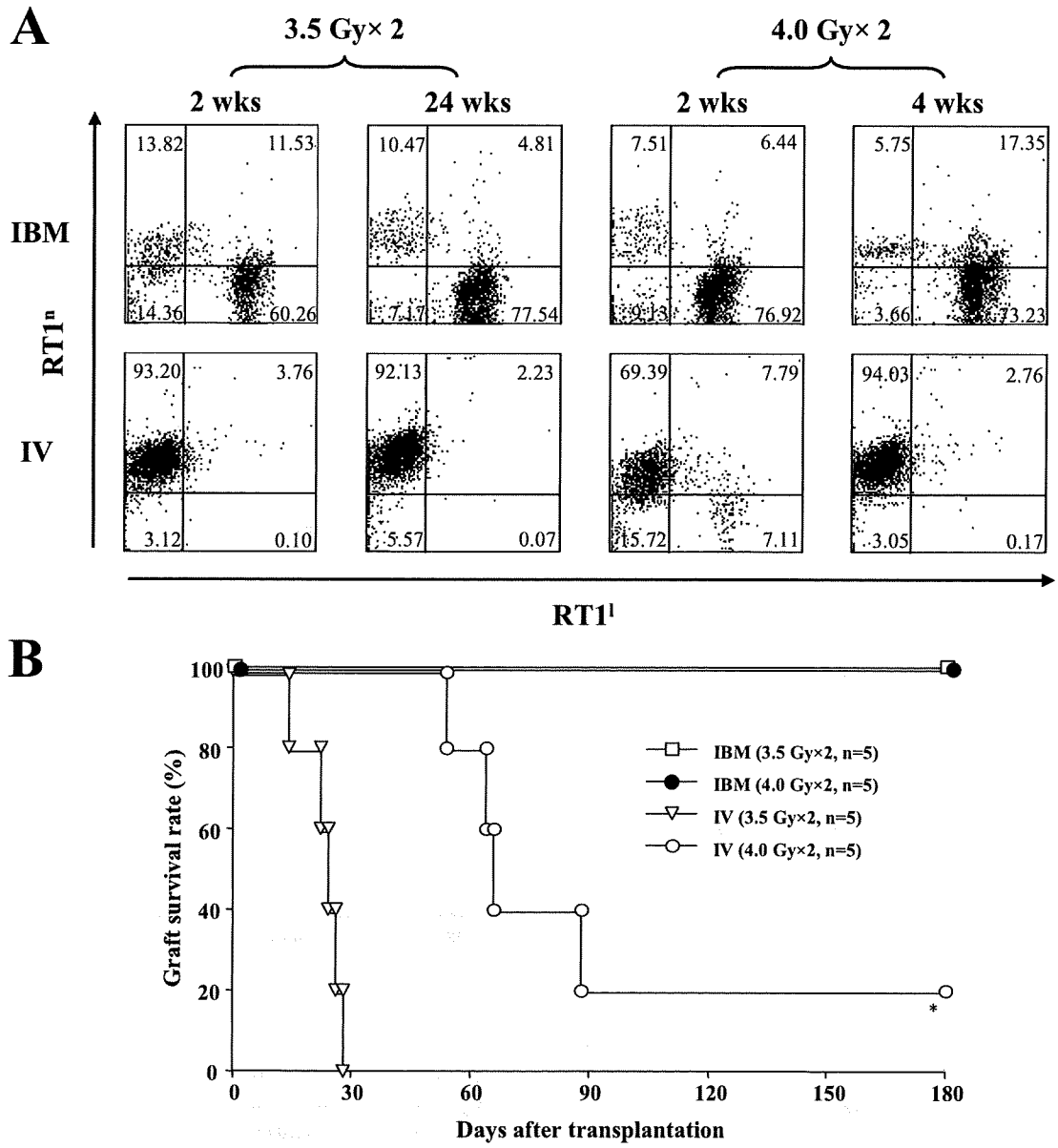

FIGURE 1. Analyses for donor-derived cells in the PBMNCs of recipients after IBM-BMT or IV-BMT. (A) PBMNCs were obtained from the recipients every 2 weeks from the 2nd to 24th week after IBM-BMT or IV-BMT plus heart transplantation, then stained with donor-specific antirat $RT1^l$ mAb (X-axis) and recipient-specific antirat $RT1^n$ mAb (Y-axis) to examine the donor cell engraftment. The stained cells were analyzed using a FACScan. FACS profiles represent representative data of five rats. Quadrants in the figures were set by the staining profile of the cells treated with isotype-matched Ig controls. Note that macrochimerism (>70%) was maintained stably after 180 days by IBM-BMT, but the transient chimerism induced by IV-BMT (fludarabine plus 4.0 Gy×2) was almost undetectable at 4 weeks. (B) Survival of cardiac allografts after IBM-BMT or IV-BMT. BN rats were injected intravenously with 50 mg/kg of fludarabine phosphate, followed by fractionated irradiation (3.5 Gy×2 or 4.0 Gy×2) 1 day before the bone marrow and heart transplantation (day −1). BMCs (3×10^7 or 10×10^7 cells/60 μL) from donor F344 rats were injected intravenously (IV-BMT) or directly into the bone marrow cavity (IBM-BMT) of the left tibia of the recipient BN rat on day 0. Vascularized heart transplantation was performed heterotopically into the right cervical portion of recipients using a microsurgical cuff technique. Allograft survival was assessed by daily palpation. Graft rejection was defined as complete cessation of spontaneous ventricular contraction.*The cardiac allograft of 1 of five rats treated with IV-BMT (4.0 Gy×2) was removed for immunohistochemical examination on day 180.

days, n=5) or within 3 months after BMT in those with fludarabine plus as much as 4.0 Gy×2 (mean survival time: 68±14.3 days, n=4) except in one instance.

Histology of Cardiac Allografts

All cardiac allografts were sectioned and stained with H-E, EvG, MT, and α-SMA mAb at the time of rejection or at

180 days after the transplantation. As already described, the cardiac allografts after IV-BMT were rejected within 1 month in the recipients conditioned with fludarabine plus 3.5 Gy×2. This was clearly confirmed by the histological findings of severe lymphocyte infiltration and extensive myocyte damage (Fig. 2D), showing evidence of acute rejection. Furthermore, despite the transient mixed chimerism induced by IV-BMT (4.0 Gy×2), severely thickened intima (cardiac allograft vasculopathy: CAV) was observed in the intramyocardial and epicardial arteries of the rejected allografts, and this was further confirmed by α-SMA staining and EvG staining (Fig. 2E). In contrast, in the allografts of the recipients conditioned with fludarabine plus 3.5 Gy×2 or 4.0 Gy×2 and treated with IBM-BMT, the arterial intima was maintained almost intact without any appearance of CAV (Fig. 2B, C).

MT staining was also performed to assess the cardiac remodeling of the allografts with respect to interstitial fibrosis during the chronic phase. While the allografts with IV-BMT (3.5 Gy×2, or 4.0 Gy×2) showed moderate to severe fibrosis in both the epicardium and intramyocardium (Fig. 2D, E and Fig. 3C, D), the prevalence of interstitial fibrosis in the allografts with IBM-BMT (3.5 Gy×2, or 4.0 Gy×2) was significantly lower than that in the allografts with IV-BMT (Fig. 2B, C and Fig. 3A, B). In addition, the coronary vessels in the allografts with IBM-BMT developed minimal myointimal thickening, compared with moderate to severe thickening with IV-BMT. Furthermore, in-

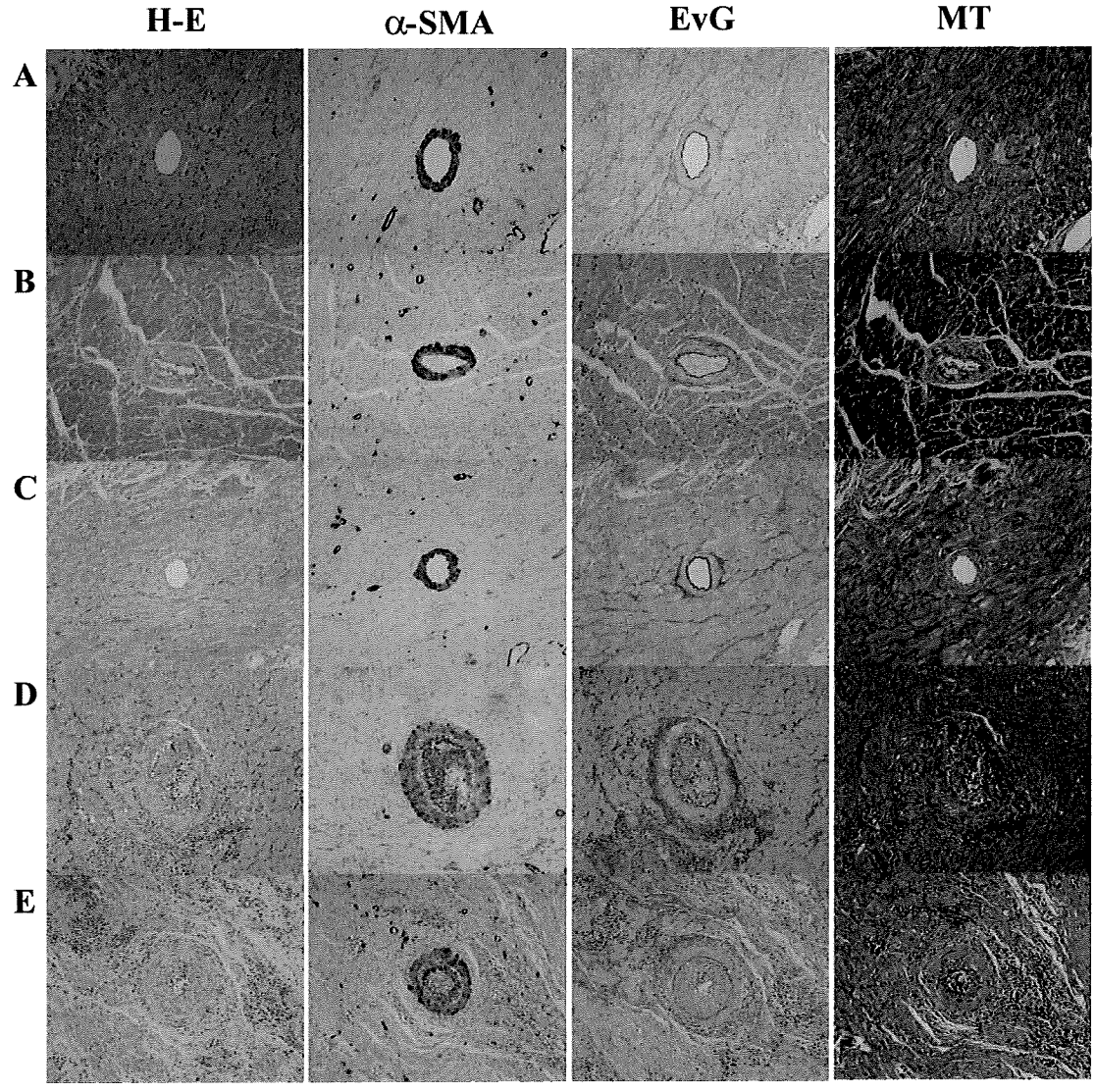

FIGURE 2. Histological findings in cardiac allografts after IBM-BMT or IV-BMT. The cardiac allografts were histologically examined at the time of rejection or 180 days after the treatment. H-E, α-SMA, EvG, or MT staining (×100) was performed to determine the rejection or the severity of CAV. (A) Intact isograft after syngeneic heart transplantation. (B) Allograft with minimal intimal thickening and sparse interstitial fibrosis at 180 days after IBM-BMT (fludarabine plus 3.5 Gy×2). (C) Allograft with well-preserved intact intima and mild interstitial fibrosis at 180 days after IBM-BMT (fludarabine plus 4.0 Gy×2). (D) Rejected allograft with severe lymphocytic infiltration and severe interstitial fibrosis at 28 days after IV-BMT (fludarabine plus 3.5 Gy×2). (E) Allograft with severe CAV and remarkable proliferation of elastic and collagenic fibers at 86 days after IV-BMT (fludarabine plus 4.0 Gy×2).

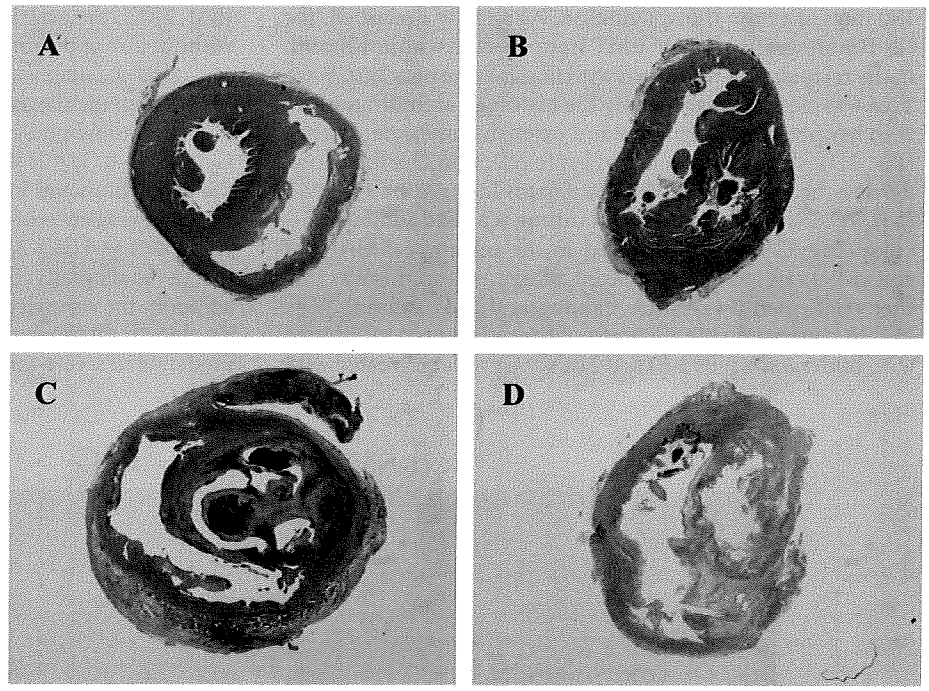

FIGURE 3. Macroscopic appearance in cardiac allografts after IBM-BMT or IV-BMT. The cardiac allografts from IBM-BMT (A, B) and IV-BMT groups (C, D) were stained with MT and coronal sections examined (×5) at the time of rejection. Allografts examined after IBM-BMT and irradiation with 3.5 Gy×2 (A) or 4.0 Gy×2 (B) showed mild interstitial fibrosis at 180 days. Allografts after the IV-BMT showed extensive interstitial fibrosis and abnormal cardiac remodeling when rejected on day 28 (3.5 Gy×2) (C) or day 86 (4.0 Gy×2) (D).

terstitial fibrosis and myocyte atrophy in the allografts with IV-BMT were significant and obvious when compared with those observed with IBM-BMT.

Analyses of Donor-Derived DCs in the Recipient Thymus

Donor-derived DCs stained with FITC-conjugated donor-specific mAb were clearly detected in the thymus of the recipient rats treated with IBM-BMT (3.5 Gy×2, and 4.0 Gy×2; Fig. 4A-C). By contrast, the presence of donor-derived DCs in the recipient thymus could not be detected in the rats treated with IV-BMT (3.5 Gy×2, or 4.0 Gy×2; Fig. 4 D-F). Therefore, regarding the long-term macrochimerism and chronic rejection-free cardiac allograft acceptance after IBM-BMT, the donor-derived DCs might interfere with the induction of donor-specific tolerance of both donor and recipient major histocompatibility complex (MHC) molecules.

Analyses of Immunological Functions

Regardless of the conditioning regimens with fludarabine plus irradiation of 3.5 Gy×2 or 4.0 Gy×2 prior to IBM-BMT, newly developed T cells were tolerant of both host-type (BN rat) and donor-type (F344 rat) MHC determinants, whereas they showed a significant response to the third-party (PVG rat) MHC determinants in MLRs (Fig. 5). In contrast, tolerance failed to be induced in the rats that had lost allografts within 3 months and also in the rat that had been sacrificed at 180 days with a weakly functioning allograft. This was further confirmed by skin grafting. The donor skin grafts were accepted (>24 weeks), whereas the third-party skin grafts from PVG rats were rejected (mean survival time: 8.4±1.5 days, n=5) in the rats treated with IBM-BMT. In contrast, the mean survival time of skin allografts in the rats treated with IV-BMT was 9.2±1.6 days (n=5) and 11.6±3.4 days (n=5) with irradiation of 3.5 Gy×2 or 4.0 Gy×2, respectively. These findings indicate that successful cooperation can be achieved among newly-developed T cells, B cells, and antigen-presenting cells in the rats treated with IBM-BMT.

Analyses of Development of GvHD

None of the rats treated with IBM-BMT or IV-BMT had any apparent body weight loss after transplantation, compared with age-matched nontreated BN rats. None of the animals showed clinical or histological evidence of GvHD throughout the period of observation (data not shown).

DISCUSSION

The major obstacles that remain in the current clinical transplantation setting include chronic rejection and side effects due to lifelong usage of nonspecific immunosuppressants (*1*). The induction of stable hematopoietic chimerism has been an attractive approach for the depletion of donor-reactive T cells in the thymus while preserving immunoreactivity against third-party antigens (*2*, *3*). The toxicity from conditioning regimens and the risk of graft failure restrict the use of conventional BMT (IV-BMT) to clinical trials for the induction of transplantation tolerance (*4*). In the present study, we demonstrated that the robust donor-specific tolerance in cardiac allografts could be readily established by simultaneously performing IBM-BMT, with less myelotoxic conditioning regimens than with IV-BMT, and free of GvHD or of the need for immunosuppressive agents after transplantation.

Similar to our previous findings in the transplantation of the leg (*12*), lung (*13*), and pancreatic islets (*14*), IBM-BMT facilitated the rapid reconstitution of donor multilineage hematolymphoid cells even when the rats were conditioned with less myelotoxic regimens than with IV-BMT. The mechanisms underlying the optimal outcome with IBM-BMT (but not with IV-BMT) may be presumed to be as follows: 1) direct injection

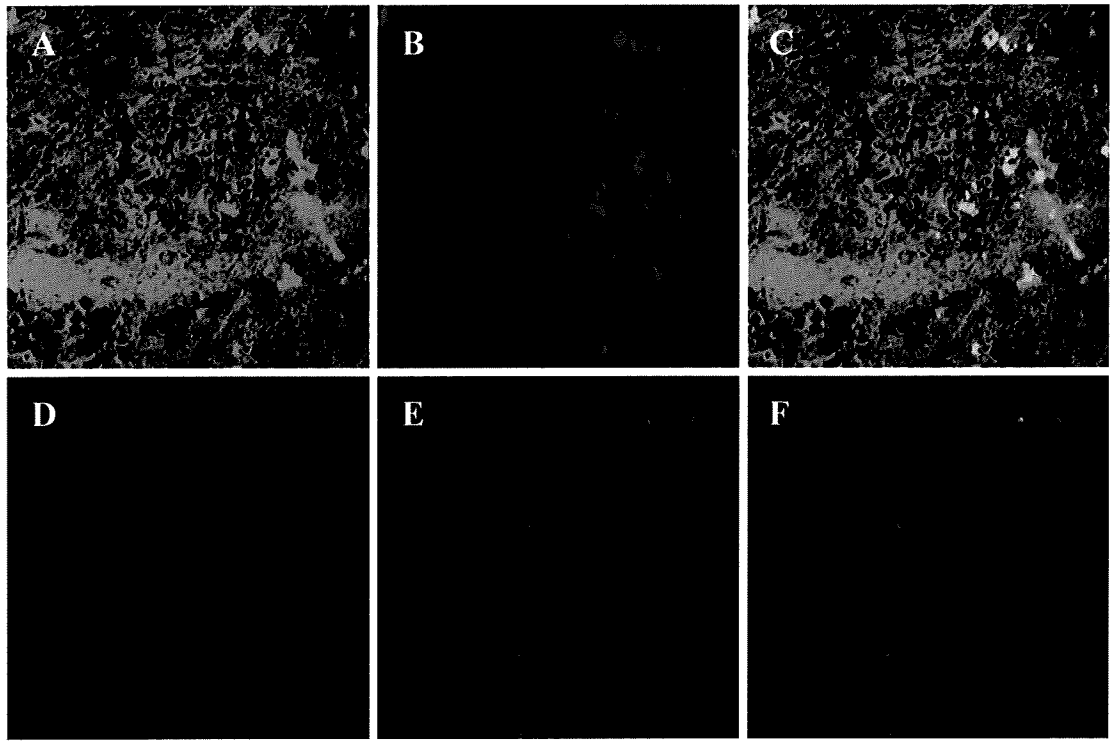

FIGURE 4. Presence of donor-derived DCs in the thymus of the rats treated with IBM-BMT or IV-BMT. Thymic sections were double-stained with FITC-antiRT1[1] mAb (A and D, cells colored green) and purified OX-62 mAb followed by PE-conjugated goat antimouse immunoglobulin G (B and E, cells colored red) for DCs and then analyzed by confocal microscopy (×200). Donor-derived DCs from the recipient rats treated with IBM-BMT were double-positive for RT1[1] and OX-62 (C, cells colored yellow); however, DCs from the recipient rats treated with IV-BMT cannot be recognized with donor-specific mAb (D, no cells colored).

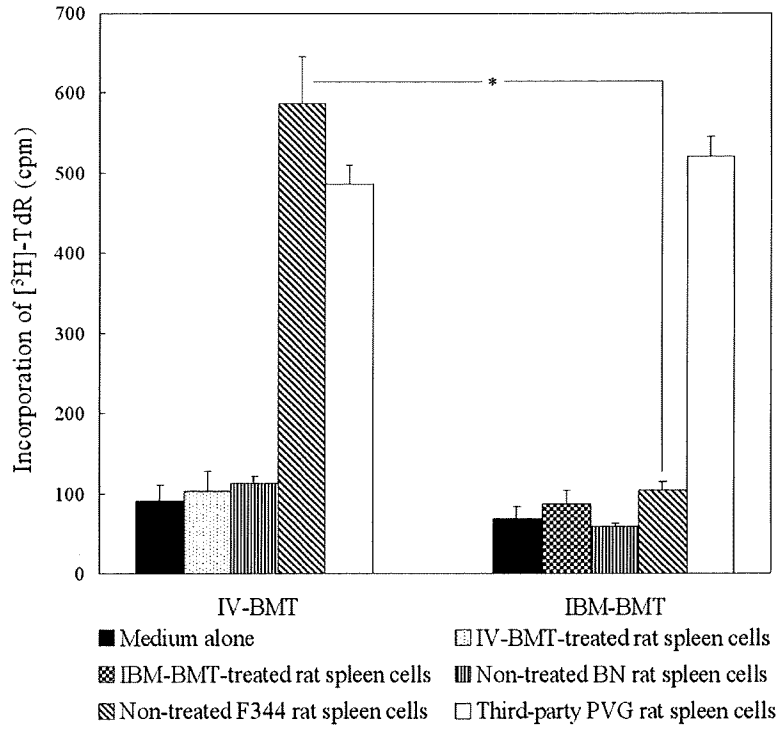

FIGURE 5. MLRs in recipient rats treated with heart transplantation plus IBM-BMT or IV-BMT. MLRs were performed 180 days after the treatment. The recipient rats treated with IBM-BMT or IV-BMT were assessed using untreated BN, F344 and PVG rats (the third party). Responder T cells (2×10^5) from the rat treated with IBM-BMT or IV-BMT were mixed with 2×10^5 stimulator cells. The results are expressed as the mean ± SD of five rats. The spleen cells from the rats treated with fludarabine+3.5 Gy×2+IBM-BMT showed tolerance of both donor-type (F344) and recipient-type (BN) MHC determinants, but showed a significant response to the third party (PVG) MHC determinants. In contrast, the spleen cells from the rats treated with fludarabine+3.5 Gy×2+IV-BMT showed significant response to donor-type (F344) MHC determinants. *$P<0.001$.

of the donor stem cells to engraftment niches without the homing process (*10*); 2) avoidance of the depletion of the antigen-disparate donor cells by the host immune system during systemic circulation (*19*); 3) donor-derived stromal cells injected into the bone marrow cavity being capable of supporting MHC-matched donor hemopoietic stem cells (HSCs) (*10, 20, 21*); and 4) injection of the donor BMCs directly into the bone marrow induces a local megadose effect, which improves the efficiency of the donor HSC engraftment, particularly under nonmyeloablative conditioning regimens (*19*). In addition, the high-dose pulse administration of fludarabine (50 mg/kg) can also facilitate the engraftment even if modest levels of irradiation are used.

The underlying mechanism by which our protocol induced hematopoietic macrochimerism and tolerance appears to involve the deletion of host alloreactive cells in both the thymus and the periphery of chimeric rats (*3*). With respect to the induction of tolerance, both the quality and quantity of the chimeric hematopoietic cells are presumed to be determinative factors (*22*). Microchimerism was first detected in some patients after solid organ transplantation due to the movement of passenger leukocytes transplanted with the graft (*23*) and was thought to be an epiphenomenon (*24*). Furthermore, acute rejection- or chronic rejection-associated graft loss has been observed in spite of microchimerism (*25*). Although many protocols achieved the acceptance of allografts via microchimerism, they often failed to sustain the long-term survival of the allografts (*26*) or failed to accept permanently fully MHC-mismatched donor skins (*9, 27*) owing to a lack of the continuous presence of bone marrow-derived donor DCs in the thymus (*28*). Therefore, the macrochimerism approach seems to be a prime strategy for the induction of transplantation tolerance, though requiring relatively stringent conditioning. In our experiments, IBM-BMT proved to be of higher efficacy in inducing persistent stable high levels of chimerism (>70%) than IV-BMT, under the mild conditioning regimens (3.5 Gy×2). Furthermore, donor-derived DCs were clearly observed in the thymus of the recipient rats after IBM-BMT but not IV-BMT (Fig. 4), indicating that bone marrow-derived donor DCs may migrate into the thymus of the chimeric rats and be involved in the induction of donor-specific tolerance. It has been reported that microchimerism does not correlate with the survival of murine cardiac allografts (*26*), and at least 30% of donor lymphocyte chimerism was found to be required to prevent rejection of allogeneic islet cells in nonobese diabetic mice (*29*). In our study, the cardiac allografts with low levels of transient chimerism were completely lost because of no use of immunosuppressants after transplantation. We hypothesize that microchimerism or low levels of chimerism may be sufficient to induce tolerance but insufficient to maintain it, particularly in the absence of immunosuppression.

Despite improvements in short-term and mid-term survival, long-term survival remains far from satisfactory in clinical heart transplantation (*30, 31*). CAV associated with chronic rejection accounts for the majority of these graft losses after operation (*32*). This lesion is known as an irreversible progressive pathogenesis and, unfortunately, the traditional immunosuppressive agents have proven to have a very limited effect except for retransplantation (*31*). At present, the only definitive treatment is known as prevention against the pathogenesis through the induction of donor-specific tolerance. Therefore, the rapid reconstitution and high levels of donor-origin hematopoietic chimerism induced by IBM-BMT might play a determinative role against CAV pathogenesis. In contrast, moderate to severe CAV and interstitial fibrosis were assessed by immunohistochemistry in the allografts treated with IV-BMT, notwithstanding the transient chimerism in the early stages.

Some recent protocols have attempted to reduce the incidence of GvHD using T-cell-depleted bone marrow. However, the chronic GvHD, engraftment failure, or opportunistic infections associated with these protocols still need to be addressed (*33*). From our previous studies, facilitating cells in the bone marrow, including $CD8^+$ T cells and stromal cells, have proven to be required for the engraftment of HSCs, especially under nonmyeloablative conditioning regimens (*34*). Martin (*35*) reported similar data where donor-derived $CD8^+$ T cells were necessary for the engraftment in autoimmune MRL/lpr mice, and the addition of a small number of donor $CD8^+$ T cells to T cell-depleted donor BMCs was capable of reconstituting recipients with donor hemopoietic cells. The graft-enhancing effect of $CD8^+$ T cells in the BMCs might be attributed to their cytotoxic or suppressive activity against host $CD8^+$ and/or $CD4^+$ T cells responsible for causing graft rejection (*36, 37*). Therefore, we injected the whole BMCs (including the facilitating cells) directly into the BM cavity. No notable differences in inducing hematopoietic chimerism between IBM-BMT and IV-BMT were observed with the injection of high doses of BMCs ($\geq 1\times10^8$) and with high doses of radiation (≥4.5 Gy×2). However, using lower doses of BMCs (3×10^7) under less myelotoxic conditioning regimens (≤4.0 Gy×2), stable high levels of macrochimerism were readily established and immunocompetence was well preserved by IBM-BMT but not by IV-BMT (Table 1). Furthermore, none of the animals that underwent IBM-BMT had clinical or histological appearance of GvHD throughout the period of observation (>10 months), which is consistent with our previous findings (*10–14*). To be of value in clinical application, IBM-BMT has proven its validity in the induction of tolerance in various immunogenic organs in rodents (*10–14*).

In conclusion, we have shown that IBM-BMT is an optimal strategy for the induction of permanent donor-specific tolerance for: 1) facilitating the establishment of stable macrochimerism with low doses of BMCs even under less myelotoxic conditioning regimens than with conventional IV-BMT; 2) inducing persistent donor-specific tolerance to allografts without acute/chronic rejection even in the absence of immunosuppressants after transplantation; and 3) reducing the incidence of GvHD even after long-term observation (>10 months). This strategy would therefore be applicable to humans.

ACKNOWLEDGMENTS

The authors thank Ms. K. Hayashi, Ms. A. Kitajima (First Department of Pathology) for their expert technical assistance, and Mr. Hilary Eastwick-Field, Mr. Brian O'Flaherty, and Ms. K. Ando for their help in the preparation of the manuscript.

REFERENCES

1. Pham SM, Kormos RL, Hattler BG, et al. A prospective trial of tacrolimus (FK506) in clinical heart transplantation: Intermediate-term results. *J Thorac Cardiovasc Surg* 1996; 111: 764.
2. Ildstad ST, Sachs DH. Reconstitution with syngeneic plus allogeneic or

xenogeneic bone marrow leads to specific acceptance of allografts or xenografts. *Nature* 1984; 307: 168.
3. Kawai T, Cosimi AB, Colvin RB, et al. Mixed allogeneic chimerism and renal allograft tolerance in cynomolgus monkeys. *Transplantation* 1995; 59: 256.
4. Buhler LH, Spitzer TR, Sykes M, et al. Induction of kidney allograft tolerance after transient lymphohematopoietic chimerism in patients with multiple myeloma and end-stage renal disease. *Transplantation* 2002; 74: 1405.
5. Gandy KL. Tolerance induction for solid organ grafts with donor-derived hematopoietic reconstitution. *Immunol Res* 2000; 22: 147.
6. Cobbold SP, Martin G, Qin S, et al. Monoclonal antibodies to promote marrow engraftment and tissue graft tolerance. *Nature* 1986; 323: 164.
7. Sykes M, Szot GL, Swenson KA, et al. Induction of high levels of allogeneic hematopoietic reconstitution and donor-specific tolerance without myelosuppressive conditioning. *Nat Med* 1997; 3: 783.
8. Wekerle T, Kurtz J, Ito H, et al. Allogeneic bone marrow transplantation with co-stimulatory blockade induces macrochimerism and tolerance without cytoreductive host treatment. *Nat Med* 2000; 6: 464.
9. Seung E, Mordes JP, Rossini AA, et al. Hematopoietic chimerism and central tolerance created by peripheral-tolerance induction without myeloablative conditioning. *J Clin Invest* 2003; 112: 795.
10. Kushida T, Inaba M, Hisha H, et al. Intrabone marrow injection of allogeneic bone marrow cells: A powerful new strategy for treatment of intractable autoimmune diseases in MRL/lpr mice. *Blood* 2001; 97: 3292.
11. Nakamura K, Inaba M, Sugiura K, et al. Enhancement of allogeneic hematopoietic stem cell engraftment and prevention of GvHD by intrabone marrow transplantation plus donor lymphocyte infusion. *Stem Cells* 2004; 22: 125.
12. Esumi T, Inaba M, Ichioka N, et al. Successful allogeneic leg transplantation in rats in conjunction with intrabone marrow injection of donor bone marrow cells. *Transplantation* 2003; 76: 1543.
13. Kaneda H, Adachi Y, Saito Y, et al. Long-term observation after simultaneous lung and intrabone marrow-bone marrow transplantation. *J Heart Lung Transplant* 2005; 24: 1415.
14. Taira M, Inaba M, Takada K, et al. Treatment of streptozotocin-induced diabetes mellitus in rats by transplantation of islet cells from two major histocompatibility complex disparate rats in combination with intra bone marrow injection of allogeneic bone marrow cells. *Transplantation* 2005; 79: 680.
15. Plunkett W, Huang P, Gandhi V. Metabolism and action of fludarabine phosphate. *Semin Oncol* 1990; 17: 3.
16. Chun HG, Leyland-Jones B, Cheson BD. Fludarabine phosphate: A synthesis purine antimetabolite with significant activity against lymphoid malignancies. *J Clin Oncol* 1991; 9: 175.
17. Goodman ER, Fiedor PS, Fein S, et al. Fludarabine phosphate: A DNA synthesis inhibitor with potent immunosuppressive activity and minimal clinical toxicity. *Am Surg* 1996; 62: 435.
18. Tomita Y, Zhang QW, Yoshikawa M, et al. Improved technique of heterotopic cervical heart transplantation in mice. *Transplantation* 1997; 64: 1598.
19. Martin PJ. Determinants of engraftment after allogeneic marrow transplantation. *Blood* 1992; 79: 1647.
20. Hashimoto F, Sugiura K, Inoue K, et al. Major histocompatibility complex restriction between hematopoietic stem cells and stromal cells in vivo. *Blood* 1997; 89: 49.
21. Wang J, Kimura T, Asada R, et al. SCID-repopulating cell activity of human cord blood-derived CD34- cells assured by intrabone marrow injection. *Blood* 2003; 101: 2924.
22. Rifle G, Mousson C. Donor-derived hematopoietic cells in organ transplantation: A major step toward allograft tolerance? *Transplantation* 2003; 75: 3S.
23. Starzl TE, Demetris AJ, Murase N, et al. Cell migration, chimerism, and graft acceptance. *Lancet* 1992; 339: 1579.
24. Manaco AP. Prospects and strategies for clinical tolerance. *Transplant Proc* 2004; 36: 227.
25. Schlitt HJ, Hundrieser J, Ringe B, et al. Donor-type microchimerism associated with graft rejection eight years after liver transplantation. *N Engl J Med* 1994; 330: 646.
26. Moraes de LV, Bueno V, Panajotopoulos N, et al. Microchimerism does not correlate with survival of murine cardiac allografts. *Transplant Proc* 2004; 36: 1021.
27. Metzler B, Gfeller P, Bigaud M, et al. Combinations of antiLFA-1, everolimus, antiCD40 ligand, and allogeneic bone marrow induce central transplantation tolerance through hemopoietic chimerism, including protection from chronic heart allograft rejection. *J Immunol* 2004; 173: 7025.
28. Tomita Y, Khan A, Sykes M. Role of intrathymic clonal deletion and peripheral anergy in transplantation tolerance induced by bone marrow transplantation in mice conditioned with a nonmyeloablative regimen. *J Immunol* 1994; 153: 1087.
29. Guo Z, Wu T, Sozen H, et al. A substantial level of donor hematopoietic chimerism is required to protect donor-specific islet grafts in diabetic NOD mice. *Transplantation* 2003; 75: 909.
30. Hosenpud JD, Bennett LE, Keck BM, et al. The registry of the international society for heart and lung transplantation: Eighteenth official report-2001. *J Heart Lung Transplant* 2001; 20: 805.
31. Waller J, Brook NR, Nicholson ML, et al. Cardiac allograft vasculopathy: current concepts and treatment. *Transpl Int* 2003; 16: 367.
32. Weis M, von Scheidt W. Coronary artery disease in the transplanted heart. *Annu Rev Med* 2000; 51: 81.
33. Ash RC, Casper JT, Chitambar CR, et al. Successful allogeneic transplantation of T-cell-depleted bone marrow from closely HLA-matched unrelated donors. *N Engl J Med* 1990; 322: 485.
34. Takeuchi K, Inaba M, Miyashima S, et al. A new strategy for treatment of autoimmune diseases in chimeric resistant MRL/lpr mice. *Blood* 1998; 91: 4616.
35. Martin PJ. Donor CD8 cells prevent allogeneic marrow graft rejection in mice: Potential implications for marrow transplantation in humans. *J Exp Med* 1993; 178: 703.
36. Tomita Y, Mayumi H, Eto M, et al. Importance of suppressor T cells in cyclophosphamide-induced tolerance to the nonH-2 encoded antigens. *J Immunol* 1990; 144: 463.
37. Asiedu C, Meng Y, Wang W, et al. Immunoregulatory role of CD8α in the effect. *Transplantation* 1999; 67: 372.

Prevention of Osteoporosis and Hypogonadism by Allogeneic Ovarian Transplantation in Conjunction With Intra-Bone Marrow–Bone Marrow Transplantation

Wei Feng,[1,4] Yunze Cui,[1,3] Changye Song,[1] Hongsheng Zhan,[4] Xiaoli Wang,[1] Qing Li,[1] Wenhao Cui,[1] Kequan Guo,[1] Masahiko Maki,[1] Hiroko Hisha,[1,2,5] Takahide Mori,[6] and Susumu Ikehara[1,2,5,7]

Background. We investigated the effects of ovarian allograft in conjunction with intra-bone marrow–bone marrow transplantation (IBM-BMT) on estrogen deficiency in mice.
Methods. Female C57BL/6 mice underwent ovariectomy (OvX). After 3 months, the mice were irradiated at 9.5 Gy, and the bone marrow cells (BMCs) of female BALB/c mice (8 weeks old) were then injected into the bone cavity of the B6 mice. Simultaneously, allogeneic ovaries from BALB/c mice were transplanted under the renal capsules of the B6 mice.
Results. Three months after the transplantation, the hematolymphoid cells were found to be completely reconstituted with donor-derived cells. The transplanted ovary tissues under the renal capsules were accepted without using immunosuppressants; there were a large number of growing follicles at different stages of development. Atrophic endometrium and its glands were also recovered by ovarian transplantation (OT). The transplanted allogeneic ovaries secreted estrogen at normal levels. Furthermore, bone loss was prevented to a certain extent.
Conclusions. These findings suggest that IBM-BMT+OT will become a valuable strategy for young women with malignant tumors to prevent premature senescence, including hypogonadism and osteoporosis, after radiochemotherapy.

Keywords: Allogeneic ovary transplantation, Intra-bone marrow–bone marrow transplantation, Ovariectomy, Osteoporosis, Hypogonadism.

(*Transplantation* 2007;84: 1459–1466)

Intensive uses of radiochemotherapy and stem cell transplantation have greatly improved the prognosis of intractable diseases such as malignant tumors in young women. Allogeneic bone marrow transplantation (BMT) has commonly been recommended in the treatment of children with relapsed or very high-risk leukemias and lymphomas today: the 10-year-survival rate after BMT is close to 50% (*1*). As the population of transplant recipients has grown, new challenges have arisen in the management of long-term complications of transplantation. Especially, the improvement of vital prognosis is frequently associated with premature ovarian failure and bone diseases. Schimmer et al. reported that all women became menopausal after BMT (*2*). A retrospective survey found that only 232 (0.6%) patients conceived after stem cell transplantation relating to 19,412 allogeneic and 17,950 autologous transplant patients (*3*). Premature ovarian failure is one of the major risk factors associated with the development of osteoporosis (*4*).

Estrogen replacement therapy is used clinically, but its risks and benefits need to be carefully weighed because of its side effects, such as the development of breast, uterine and ovarian cancers, and heart diseases, especially in young women with premature ovary failure (POF) who

This study was supported by grants from the Haiteku Research Center of the Ministry of Education; the Millennium, Science Frontier, and the 21st Century Center of Excellence programs of the Ministry of Education, Culture, Sports, Science and Technology; Health and Labour Sciences; the Department of Transplantation for Regeneration Therapy (sponsored by Otsuka Pharmaceutical Company); the Molecular Medical Science Institute (Otsuka Pharmaceutical Company); Japan Immunoresearch Laboratories; the Medical Academia for Reproductive Regeneration; the National Natural Science Foundation of China (30371793); and the Shanghai Leading Academic Discipline Project (T0303).

[1] First Department of Pathology, Kansai Medical University, Moriguchi City, Osaka, Japan.
[2] Department of Transplantation for Regeneration Therapy, Kansai Medical University, Moriguchi City, Osaka, Japan.
[3] Japan Immunoresearch Laboratories, Gunma, Japan.
[4] Shuguang Hospital, Shanghai University of Traditional Chinese Medicine, Shanghai, China.
[5] Regeneration Research Center for Intractable Diseases, Kansai Medical University, Moriguchi City, Osaka, Japan.
[6] Medical Academia for Reproductive Regeneration, Kyoto, Japan.
[7] Address correspondence to: Susumu Ikehara, M.D., Ph.D., First Department of Pathology, Kansai Medical University, 10–15 Fumizono-cho, Moriguchi City, Osaka 570-8506, Japan.
E-mail: ikehara@takii.kmu.ac.jp
Received 4 May 2007. Revision requested 9 July 2007.
Accepted 26 August 2007.

ISSN 0041-1337/07/8411-1459
DOI: 10.1097/01.tp.0000288182.75398.74

need to use exogenous estrogen for a long time (*5–7*). If endogenous estrogen can be provided, it may solve the problem of side effects resulting from long-term estrogen replacement therapy.

We have recently found that intra–bone marrow BMT (IBM-BMT) is so far the best strategy for allogeneic BMT (*8*). IBM-BMT creates an appropriate hemopoietic environment for the early recovery of hemopoiesis and donor cell engraftment, since BMCs collected by the perfusion method contain not only hemopoietic stem cells (HSCs) but also mesenchymal stem cells (MSCs) (*9*), and IBM-BMT can efficiently recruit both (*8*). We have also shown that IBM-BMT can be used for organ transplantation because it allows us to reduce irradiation doses as the conditioning regimen (*10–12*).

In the present study, we attempt to treat secondary hypogonadism and osteoporosis by IBM-BMT plus ovarian transplantation (OT). We here show that IBM-BMT+OT can be used to treat patients with secondary ovarian failure and osteoporosis.

MATERIALS AND METHODS

Animals

Female 8-week-old C57BL/6 (B6: H-2K^b) mice, BALB/c mice (H-2K^d), and C3H/HeN mice (as third party) were purchased from SLC (Shizuoka, Japan). These mice were maintained in our animal facilities under specific pathogen-free conditions until use. Mice had ad libitum access to water and commercial standard food.

Experimental Protocols

The female C57BL/6 (B6: H-2K^b) mice were divided into four groups with eight mice per group. In brief, there was a sham-operated group (Sham-operated), OvX group, OvX+IBM-BMT group and OvX+IBM-BMT+OT group, according to a randomized block design using body weight as a selection parameter. At the begining of the experiment, three groups underwent OvX (*13*) bilaterally under diethyl ether anesthesia, and the remaining group (intact) was sham-operated. After 3 months, two groups of OvX mice were lethally irradiated at 9.5 Gy, and 1 day after the irradiation, the mice were transplanted with whole BMCs (1×10^7 /10 μL/mouse) from female BALB/c mice (H-2K^d, female 8 weeks old) via IBM injection. Allogeneic bone marrow cells were then injected into the left tibia bone cavity, and each mouse in one group was simultaneously transplanted an allogeneic ovary under its renal capsule. Another group served as an only IBM-BMT control group. After 3 months of treatment, mice were killed by cervical dislocation, weighted their uterus and body, and blood was removed by cardiac puncture. Serum was stored at −80°C for further analysis (Fig. 1A).

All of the bright-field images were taken on an Olympus BH-2 microscope (Olympus Optical, Tokyo, Japan) with a Fujifilm HC-2500 digital camera (Fujifilm, Tokyo, Japan) and Photograb-2500 software.

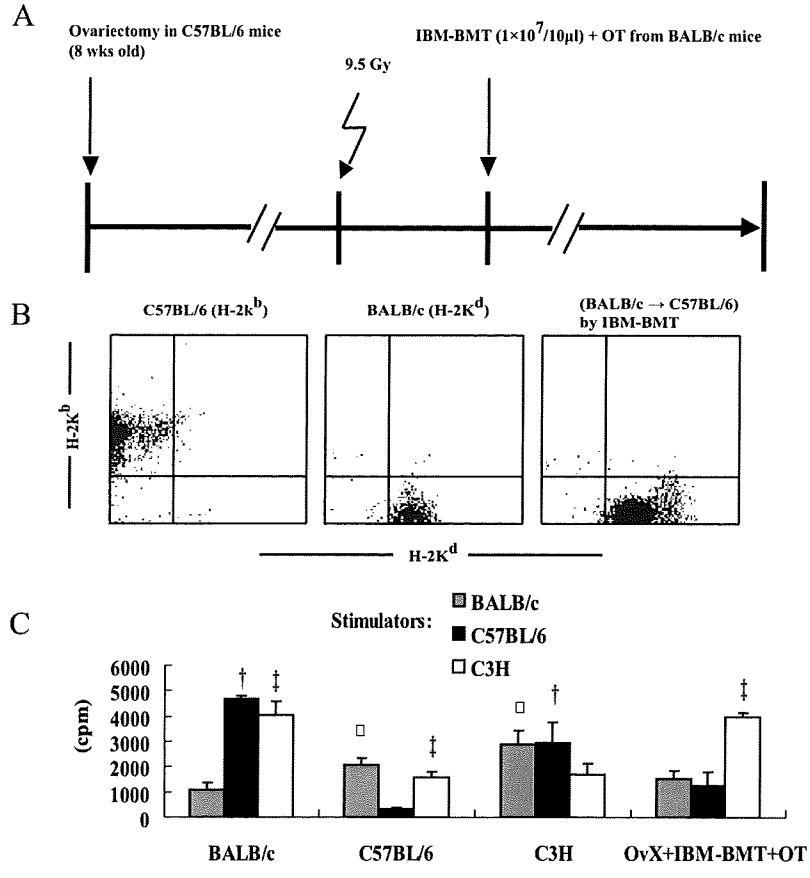

FIGURE 1. OvX mice treated with IBM-BMT. B6 mice at the age of 8 weeks were OvX. After 3 months, the mice were irradiated with a lethal dose (9.5 Gy), and BMCs from normal BALB/c mice were injected directly into the bone marrow cavity (IBM-BMT) of the left tibia (A). Three months after IBM-BMT and OT, cells from the peripheral blood of chimeric mice were stained with FITC-conjugated anti–H-2K^b mAb (recipient type) or anti–H-2K^d mAb (donor type). Cells from C57BL/6 mice treated with IBM-BMT from BALB/c mice were donor origin (H-2K^d). These findings indicate that the hemopoietic cells were reconstituted with donor-type cells after IBM-BMT (B). Mixed leukocyte reactions: Responder cells (4×10^5) were cultured with 3×10^5 irradiated (15 Gy) stimulator cells for 96 hr and pulsed with 0.5 μCi of [^{3}H]-thymidine for the last 18 hr of the culturing period (C). Cultures were performed in triplicate. Data are expressed as mean±SD, n=3. $^{\square}P<0.01$ vs. BALB/c; $^{\dagger}P<0.01$ vs. C57BL/6; $^{\ddagger}P<0.01$ vs. C3H.

Preparation and Inoculation of BMCs

Bone marrow cells were collected from the femurs and tibias of BALB/c mice. In brief, Donor BMCs from female BALB/c mice were flushed from tibiae, femurs, and humeri using Roswell Park Memorial Institute (RPMI) 1640 medium (Niken CM1101, Japan) supplemented with 2% heat-inactivated fetal calf serum (PAA.A15–001; Austria) on ice. BMCs were filtered through a sterile nylon mesh, resuspended in sterile phosphate-buffered saline. IBM-BMT injection was carried out according to the method described previously (*9*). In brief, the knee was flexed to 90 degrees and the proximal side of the tibia was drawn to the anterior. A 26-gauge needle was inserted into the joint surface of the left tibia through the patellar tendon and then inserted into the bone marrow (BM) cavity of the left tibia. Using a microsyringe (50 μL; Hamilton Company, Reno, NV), the donor BMCs (1×10^7/10 μL/mouse) were injected into the BM cavity.

Flow Cytometry

BMCs, spleen cells, and peripheral blood cells were prepared from the recipient mice after three months with bone marrow transplantation, followed by red blood cell lysis with ammonium chloride (8.3 g/ml; Sigma-Aldrich, St. Louis, MO). To detect donor- or residual recipient-derived cells, the cells were stained with fluorescein isothiocyanate (FITC)–conjugated anti–H-$2K^d$ and phycoerythrin (PE)–conjugated anti-H-$2K^b$ monoclonal antibodies (mAbs; PharMingen, San Diego, CA). The cells were analyzed using a FACScan (Becton, Dickinson and Company, Mountain View, CA).

Mixed Leukocyte Reaction

Mixed leukocyte reaction (MLR) was performed as follows: splenic T cells (derived from normal C57BL/6, BALB/c, C3H mice and OvX+IBM-BMT+OT mice) were isolated by mechanical dissociation using microscope slides followed by red blood cell lysis with ammonium chloride (8.3 g/ml; Sigma-Aldrich). The 4×10^5 responder T cells were cultured with 4×10^5 or 3×10^5 irradiated (15 Gy) stimulator spleen cells for 96 hr in 10% FBS RPMI with 50 μM 2-ME, then pulsed with 0.5 μCi of [^{3}H]-thymidine for the last 18 hr of the culturing period.

Histology of Bone

Vertebras were fixed in 10% formalin and then decalcified and paraffin-embedded. The lumbar vertebra was sectioned to obtain a longitudinal midline section through the vertebral body, and then the sections were stained with hematoxylin and eosin (H&E). Left tibias of mice were removed the soft tissues, stored in 70% ethanol for peripheral quantitative computed tomography (pQCT) analysis. Bone histomorphometry and pQCT were used to evaluate bone mass. Percentage of trabecular bone area (B.Ar/T.Ar) was used to evaluate bone mass in histomorphometry: the fourth lumbar vertebra of every sample was cut into five consecutive sections, and these sections were measured by image analysis software (Lumina vision 1 image analysis system, Japan). A small animal pQCT (XCT Research SA, Stratec Medizjntechnik, Pforzheim, Germany) was used for the measurements. When detected, bone was fixed in plastic tube (8-mm diameter) with a spring and scanned with pQCT equipment (XCT 540; Stratec). For the measurement levels in tibia, the reference line was placed at the proximal end of the bone. Three cross-sections, at 0.3-mm intervals, were analyzed 1.8 mm from the reference line. Measurements were also taken from two sections separated by 1 mm, starting 2.5 mm above a reference line at the tibiofibular junction. Special Software version 5.40 (Stratec) was used to analyze the images of each section, with a voxel size of 0.10 mm. The total bone mineral densities (BMD) of the proximal tibia were applied for BMD analyses.

Histology of Ovary and Uterus

Three months after IBM-BMT, the uteri, and their ovary, including the allogeneic ovary transplanted under the renal capsules were removed, weighed and then fixed in 10% formalin. The sections were stained with H&E to observe ovarian and uterine morphology.

Serum Estradiol Levels

Serum specimens were collected from the treated and nontreated B6 mice, Serum samples were separated by centrifugation and stored at −80°C until used for measurements. Serum estradiol was quantified by an enzyme-linked immunosorbent assay (ELISA) kit (IBL-Hamburg GmbH Corp., Hamburg, Germany).

Urine Deoxypyridinoline (DPD) Analyses

Urine specimens were collected from the treated and nontreated B6 mice, stored at −80°C until used for measurements. The urinary DPD was quantified by an ELISA kit (Quidel Corp., San Diego, CA) to evaluate the bone loss.

Statistical Analyses

All data were presented as mean±SD. Significance of the results was determined by two-way analysis of variance. Differences were calculated by Students *t* test. A *P* value <0.01 was considered statistically significant.

RESULTS

In our preliminary experiments, we compared the survival rates of chimeric mice (BALB/c→B6) treated with conventional BMT (intravenous injection of bone marrow cells: IV-BMT) with those treated with IBM-BMT. IV-BMT-treated chimeric mice showed significantly shorter survival than IBM-BMT-treated chimeric mice, although those mice in the IV-BMT-treated group that did survive showed full chimerism (>98% donor type); we used a lethal irradiation dose (9.5 Gy) in this experiment to examine the effects of irradiation on osteoporosis and ovarian dysfunction. Therefore, in the present study (as shown in Fig. 1A), we first ovariectomized B6 mice (8 weeks old) and, 3 months later, irradiated them with 9.5 Gy. They received IBM-BMT (instead of IV-BMT) the day after the irradiation.

Cell Surface Antigens

Three months after IBM-BMT, we carried out flow cytometrical analyses using BMCs, spleen cells and peripheral blood cells obtained from the recipient mice and examined the engraftment of donor-derived cells. The percentages of

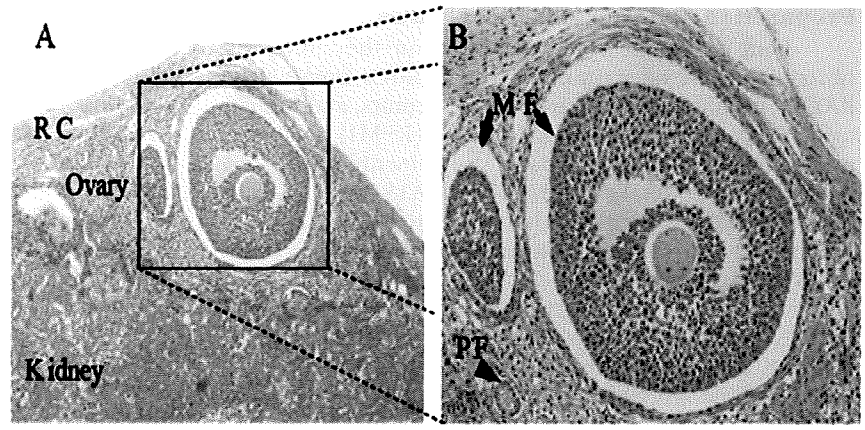

FIGURE 2. Histology of transplanted ovary after IBM-BMT. Three months after IBM-BMT and OT, the ovary was accepted (original magnification ×100, A) with a large number of mature follicles (MF) and primary follicles (PF) (original magnification×200, B) under the renal capsule (RC).

donor (BALB/c) – derived cells (H-2k^d) in the peripheral blood (Fig. 1B), BM, and spleen are 99.23%, 99.69%, and 99.54%, respectively.

Immunological Functions

We performed mixed lymphocyte reaction (MLR) using T cells as a responder obtained from the spleen of IBM-BMT-treated mice. Newly-developed T cells, as shown in Figure 1C, were tolerant of both host (C57BL/6)-type and donor (BALB/c)-type major histocompatibility complex (MHC) determinants, whereas they showed normal responses to the third-party (C3H) cells.

Histology and Weight of Ovary and Uterus

Three months after IBM-BMT+OT, the mice were sacrificed and confirmed that allogeneic ovaries had been accepted under the renal capsules of B6 mice (Fig. 2). In the mice, there were a large number of growing follicles in different stages of development, such as mature follicles, primary follicles and primordial follicles. The uteri showed normal endometrium including endometrial glands. However, in the OvX+IBM-BMT group (without OT), the uteri showed atrophic endometrium and few endometrial glands (Fig. 3A). Uterus/body weight ratios significantly increased in the OvX+IBM-BMT+OT group, compared with the OvX+IBM-BMT group or the OvX group (Fig. 3B). Uterine weight also increased in the OvX+IBM-BMT+OT group, compared with the OvX+IBM-BMT group. These results indicate that OT leads to the secretion of estrogen and restores uterine growth in the OvX mice.

Bone Histology

In the OvX+IBM-BMT+OT group, the sections of a lumbar vertebral-4 (L4) body showed that trabeculae number, thickness, and longness increased, in comparison with the OvX+IBM-BMT group, indicating that bone loss was prevented, while, in the OvX+IBM-BMT group, trabeculae were thin, and trabecular numbers decreased in comparison with the OvX group, the OvX+IBM-BMT+OT group, and the sham-operated group (Fig. 4). Histomorphometry and bone mineral densitometry were utilized to assess the bone mass of lumbar vertebrae and tibiae, respectively. The percentages of trabecular bone area (B.Ar/T.Ar) of lumbar vertebrae in the OvX+IBM-BMT+OT group increased significantly, compared with the OvX+IBM-BMT group. The total BMD of the proximal tibia are determined with pQCT. After IBM-BMT, the OT group maintained their mass, while the bone mass in the OvX+IBM-BMT group rapidly decreased; there were significant differences between the OvX group and the OvX+IBM-BMT+OT group. These results indicated that bone mass was maintained and increased after allogeneic OT, and that total body irradiation as a conditioning regimen for transplantation has toxic effects on the bone (Table 1).

Levels of Serum Estradiol and Urine DPD

There were no statistical differences between the sham-operated group and the OvX+IBM-BMT+OT group in the serum estrogen levels, suggesting that allogeneic ovaries transplanted under the kidney capsules were accepted and could secrete estrogen, resulting in maintaining normal estrogen levels in the OvX mice. The estrogen levels in the OvX+IBM-BMT group were the lowest in the three experimental groups; the OvX group was similar to the OvX+IBM-BMT group, while there was a significant difference between the OvX group and the OvX+ IBM-BMT+OT group. The levels of DPD released from the breakdown of collagen were measured in the urine to estimate osteoclast activity. The DPD levels in the OvX+IBM-BMT+OT group decreased, indicating that bone resorption decreased and bone turnover rate by OvX was suppressed after allogeniec OT. In the OvX+IBM-BMT group, however, the DPD levels were high, indicating that bone loss could not be prevented without OT (Table 2).

DISCUSSION

More and more cancer patients will be long-term survivors of radiochemotherapy and BMT, but a long lifespan does not necessarily imply a normal life. Especially in young women, ovarian failure and premature menopause have a strong impact on self-esteem and quality of life (*14–17*). Therefore, the lasting adverse effects of these modalities are receiving increasing attention.

Research during the last decade has revealed that estrogen regulates bone homeostasis through direct effects on bone cells. Estrogen deficiency results in an uncoupling of bone remodeling with a marked increase in bone resorption compared with bone formation.

Initiation of estrogen replacement therapy (ERT) in experimental animals and humans decreases erosion depth and

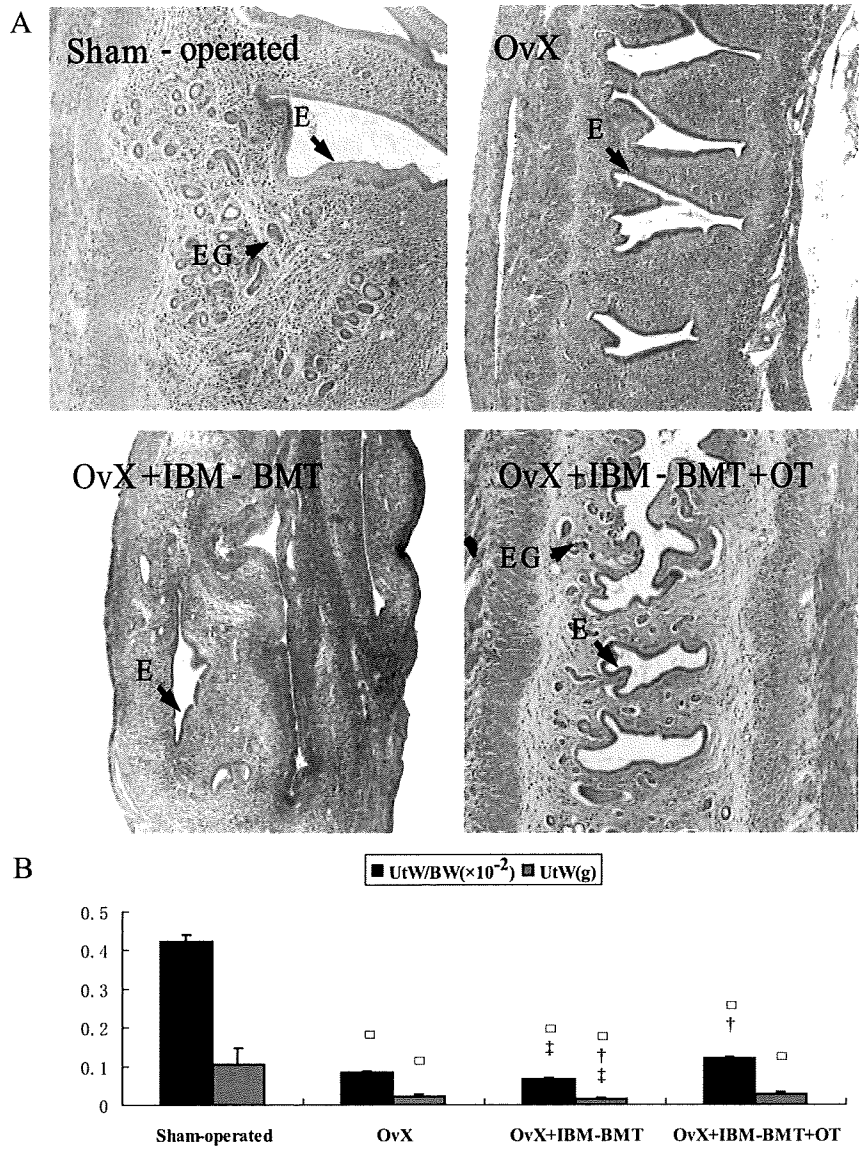

FIGURE 3. FEffects of IBM-BMT with OT on uterus. Three months after IBM-BMT, uteri of four groups (sham-operated group, OvX group, OvX+IBM-BMT group, and OvX+IBM-BMT+OT group) were sectioned and stained with hematoxylin and eosin. The OvX+IBM-BMT+OT group's uteri revealed normal endometrial glands (EG) and endometrium (E) morphology, but the other two experimental groups' uteri, especially the OvX+IBM-BMT group's uteri, revealed atrophic endometrium and few endometrial glands. Original magnification: ×100 for all panels (A). Uterus/body weight ratio and uterus weight were measured in the sham-operated group, OvX group, OvX+IBM-BMT+OT group, and OvX+IBM-BMT group. Data are expressed as mean ±SD, n=8. □$P<0.01$ vs. sham-operated group; †$P<0.01$ vs. OvX group; ‡$P<0.01$ vs. OvX+IBM-BMT+OT group (B).

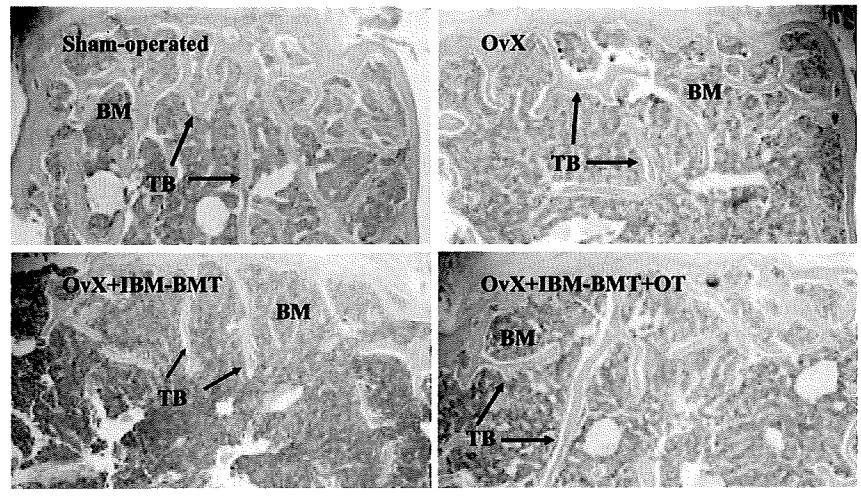

FIGURE 4. Histology of the lumbar vertebrae after IBM-BMT. Three months after IBM-BMT, the 4th lumbar vertebrae of mice in each of the four groups (sham-operated group, OvX group, OvX+IBM-BMT group, and OvX+IBM-BMT+OT group) were sectioned and stained with hematoxylin and eosin. Significant loss of trabecular bone (TB) was observed in the OvX group and the OvX+IBM-BMT groups; the trabeculars in the OvX+IBM-BMT group were short and small, but there were longer trabecular bones in the OvX+IBM-BMT+OT group. Original magnification: ×40 for all panels. BM, bone marrow.

TABLE 1. Effects of IBM-BMT with OT on L4 trabecular bone area and proximal tibia BMD in OvX mice

Group	L4 trabecular bone area percent (B.Ar/T.Ar)	Proximal tibia BMD (mg/cm^3)
Sham-operated	28.03±4.68	512.75±21.87
OvX	10.64±2.41[a]	445.58±27.61[a]
OvX+IBM-BMT	7.53±1.72[a,b,c]	336.97±71.45[a,b,c]
OvX+IBM-BMT+OT	15.18±1.83[a,b]	442.10±29.34[a]

The OvX mice were treated for 3 months, and the L4 trabecular bone area and proximal tibia BMD were then measured by histomorphometry and pQCT, respectively. The trabecular bone area and proximal tibia BMD of the OvX+IBM-BMT+OT group increased, compared with the OvX+IBM-BMT group, indicating that bone formation increased. Data are expressed as means± SD, n=8.

[a] $P < 0.01$ vs. sham-operated group.

[b] $P < 0.01$ vs. OvX group.

[c] $P < 0.01$ vs. OvX+ IBM-BMT+OT group.

B.Ar/T.Ar, bone area/total area.

TABLE 2. Effects of IBM-BMT with OT on serum estrogen and urinary deoxypiridinoline (DPD) in OvX mice

Group	Serum estrogen (pg/mL)	Urinary DPD (nM)
Sham-operated	7.88±2.09	8.57±3.42
OvX	4.59±1.66[a]	14.01±6.28[a]
OvX+IBM-BMT	1.77±1.19[a,b,c]	18.95±6.16[a,b,c]
OvX+IBM-BMT+OT	7.69±1.71[b]	11.41±3.91[a]

Serum estrogen and urinary DPD were measured using ELISA kit. There were no significant differences between the sham-operated group and the OvX +IBM-BMT+OT group in serum estrogen assay. The hormonal rise indicated functioning allografts. In the DPD assay, the DPD level of the OvX+IBM-BMT+OT group declined compared with the OvX+IBM-BMT group, indicating that bone resorption decreased. Data are expressed as means± SD, n=8.

[a] $P < 0.01$ vs. sham-operated group.

[b] $P < 0.01$ vs. OvX group.

[c] $P < 0.01$ vs. OvX+IBM-BMT+OT group.

osteoclast activation frequency by stimulating apoptosis and blocking osteoclastogenesis (*18*). Estrogen therapy may decrease the rate of bone turnover by about 50% in the adult, resulting in fracture reduction at the spine, hip, and other sites of between 30% and 50% (*19*, *20*). However estrogen needs to be given for as long as the effect is required, within a few years of stopping hormone replacement therapy (HRT), the antifracture effect is no longer present (*21*).

The limitations in the use of estrogen are a consequence of the adverse effects. The Women's Health Initiative and The Million Women Study found an increased risk of stroke, coronary heart disease, and breast cancer associated with long-term treatment with HRT (*19*). Young women with premature ovarian failure need estrogen therapy for longer than older women, with the result that the adverse effects of exogenous estrogen will be more severe.

In this study, we carried out allogeneic IBM-BMT+OT on OvX mice to investigate the effects of endogenous estrogen secreted by allogeneic ovary, since we have recently proven in many animal experiments that different kinds of donor cells including HSCs could be efficiently recruited into the bone marrow by IBM-BMT, which leads to the rapid hemopoietic and immune recovery of recipients, inducing donor-specific tolerance in allogeneic organ transplantation, and promoting the survival rate of recipients (*8*, *9*).

In the present study, three months after the transplantation, the hematolymphoid cells were found to be completely reconstituted with donor-derived cells. The transplanted ovary tissues under the renal capsules were accepted without using immunosuppressants; even after 10 months, mature follicles were found in the allogeneic ovary engrafted after IBM-BMT without using any immunosupressants. The levels of endogenous estrogen were no different between the OvX+IBM-BMT+OT group and normal control group (sham-operated group). We know that irradiation can result not only in ovarian failure, but also in uterine dysfunction. However, in the present study, after IBM-BMT+OT, the ratio of uterus/body weight and uteri weight increased in the OvX+IBM-BMT+OT group. Moreover, endometrial morphology including endometrial glands was almost normal, although the uterine volume was still below the normal range. In another experiment, female mice without OvX received allogeneic IBM-BMT and allogeneic OT under the renal capsule after lethal irradiation. After 3 months, many immature follicles remained in the recipients' ovaries. It is well known that gonads are radiosensitive; low-dose irradiation can completely sterilize female mice. The immature follicles that remained in the recipients' ovaries had probably developed from germline stem cells (GSCs) residing in the recipients' ovaries (*22*) or from bone marrow (*23*) after IBM-BMT+OT. Also, after allogeneic IBM-BMT+OT as described above, in one group of mice we used the Johnson protocol (*22*) to transplant the allogeneic ovaries into the recipient's bursal cavity in contact with the remaining host ovarian. These mice were then mated with male mice. Two of 8 mice achieved pregnancy (data not shown). We therefore believe that IBM-BMT + OT may help promote the reconstitution of uterine functions.

The dominant acute effect of estrogen is the blockade of new osteoclasts formation. Osteoclasts arise by cytokine-driven proliferation and differentiation of monocyte precursors that circulate within the hematopoietic cell pool (*24*). This process is facilitated by bone marrow stem cells, which provide physical support for nascent osteoclasts and produce soluble and membrane-associated factors essential for the proliferation and differentiation of osteoclast precursors.

IBM-BMT can facilitate the early engraftment of hematopoietic cells of donor origin (*8*, *9*), indicating that it can generate normal osteoclasts in the bone marrow. As has been recently reported, BMCs contain not only HSCs (including osteoclast precursors), but also MSCs (including osteoblasts) (*25*). BM stromal cells can differentiate into osteoblasts, chondrocytes, adipocytes, cardiomyocytes, and even neurons (*26–28*). By IBM-BMT, not only donor-derived HSCs but also donor-derived MSCs can be recruited into the bone marrow site and can proliferate and differentiate. Estrogen can directly modulate the differentiation of bone marrow stromal cells into osteoblasts and increase the deposition and mineralization of matrix (*29*, *30*).

In the present study, mice were first ovariectomized to precipitate a marked reduction in endogenous estrogen con-

centrations and to induce bone remodeling abnormalities that augment bone loss and increase the risk of developing osteopenia or osteoporosis. We found that the bone mass in the OvX+IBM-BMT+OT group showed a significant increase after 3 months, while DPD as a biochemical bone resorption marker decreased compared with the OvX+IBM-BMT group, although the BMD did not regain the normal levels, in contrast to the sham-operated group. In another experiment, we noted that the bone mineral density of the OvX+IBM-BMT+OT group did not increase even after 6 months, compared with 3 months in the present experiment (data not shown). Lee youngwon et al. showed that the differentiation of bone marrow stromal cells into osteoblasts was impaired after BMT (*31*). On the other hand, Wang et al. reported that MSC transplantation can help to strengthen osteoporotic bone (*32*) without using irradiation as the conditioning regimen. Thus, the toxic effect of total body irradiation (TBI) on the bone is so severe and complicated (*33*, *34*) that we think both antiosteoporotic effects of endogenous estrogen secreted by the transplanted ovary and donor-derived MSCs were insufficient to establish normal BMD in 3 months; nonmyeloablative conditioning regimens may be substituted for TBI in future. We suggest that antiosteoporotic drugs are used as soon as possible after ovarian failure, and before and after BMT in clinical practice to prevent bone loss.

Many antiosteoporotic drugs are used to prevent and treat postmenopausal osteoporosis, but they do not have curative effects on symptoms such as hot flashes and the urogenital complaints induced by endogenous estrogen deficiency besides HRT (*35*, *36*).

From our results, we believe that IBM-BMT plus ovarian allografts would be advantageous for young women with primary or secondary estrogen deficiency (due to chemotherapy and radiation therapy in malignant diseases). Transplantation surgery is limited by the supply of fresh donor organs. It has been reported that cryopreserved intact ovary grafts succeeded in syngeneic rats (*37*). We believe that, if this new strategy can be shown to be safe for application to humans, IBM-BMT+OT could not only be used to treat cancer and prevent bone loss, but could also help promote the patient's self-esteem and quality of life.

ACKNOWLEDGMENTS

We thank Ms. Y. Tokuyama, K. Hayashi and A. Kitajima for their expert technical assistance. We also thank Mr. Hilary Eastwick-Field and Ms. K. Ando for their help in the preparation of the manuscript.

REFERENCES

1. Larsen EC, Loft A, Holm K, et al. Oocyte donation in women cured of cancer with bone marrow transplantation including total body irradiation in adolescence. *Hum Reprod* 2000; 15: 1505.
2. Schimmer AD, Quatermain M, Imrie K, et al. Ovarian function after autologous bone marrow transplantation. *J Clin Oncol* 1998; 16: 2359.
3. Salooja N, Szydlo RM, Socie G, et al. Pregnancy outcomes after peripheral blood or bone marrow transplantation: A retrospective survey. *Lancet* 2001; 358: 271.
4. Alper MM, Garner PR. Premature ovarian failure: Its relationship to autoimmune disease. *Obstet Gynecol* 1985; 66: 27.
5. Davis SR. Premature ovarian failure. *Maturitas* 1996; 23: 1.
6. Haukvik UKH, Dieset I, Bjøro T, et al. Treatment-related premature ovarian failure as a long-term complication after Hodgkin's lymphoma. *Ann Oncol* 2006; 17: 1428.
7. Notelovitz M. Clinical opinion: The biologic and pharmacologic principles of estrogen therapy for symptomatic menopause. *Med Gen Med* 2006; 288: 85.
8. Ikehara S. Intra-bone marrow-bone marrow transplantation: A new strategy for treatment of stem cell disorders. *Ann N Y Acad Sci* 2005; 1051: 626.
9. Kushida T, Inaba M, Hisha H, et al. Intra-bone marrow injection of allogeneic bone marrow cells: A powerful new strategy for treatment of intractable autoimmune diseases in MRL/lpr mice. *Blood* 2001; 97: 3292.
10. Jin T, Toki J, Inaba M, et al. A novel strategy for organ allografts using sublethal (7 Gy) irradiation followed by injection of donor bone marrow cells via portal vein. *Transplantation* 2001; 71: 1725.
11. Taira M, Inaba M, Takada K, et al. Treatment of streptozotocin-induced diabetes mellitus in rats by transplantation of islet cells from two major histocompatibility complex disparate rats in combination with intra bone marrow injection of allogeneic bone marrow cells. *Transplantation* 2005; 79: 680.
12. Esumi T, Inaba M, Ichioka N, et al. Successful allogeneic leg transplantation in rats in conjunction with intra-bone marrow injection of donor bone marrow cells. *Transplantation* 2003; 76: 1543.
13. Waterhouse T, Cox SL, Snow M, et al. Offspring produced from heterotopic ovarian allografts in male and female recipient mice. *Reproduction* 2004; 127: 689.
14. Schover L. Sexuality and body image in younger women treated for breast cancer. *J Natl Cancer Inst Monog* 1997; 16: 177.
15. Brenner PF. The menopausal syndrome. *Obstet Gynecol* 1988; 72: 68.
16. Ganz PA, Greendale GA, Petersen L, et al. Breast cancer in younger women: reproductive and late health effects of treatment. *J Clin Oncol* 2003; 21: 4184.
17. Ganz PA, Rowland JH, Desmond K, et al. Life after breast cancer: understanding women's health-related quality of life and sexual functioning. *J Clin Oncol* 1998; 16: 501.
18. Eriksen EF, Langdahl B, Vesterby A, et al. Hormone replacement therapy prevents osteoclastic hyperactivity: A histomorphometric study in early postmenopausal women. *J Bone Miner Res* 1999; 14: 1217.
19. Rossouw JE, Anderson GL, Prentice RL, et al. Risks and benefits of estrogen plus progestin in healthy postmenopausal women: Principal results from the Women's Health Initiative randomized controlled trial. *JAMA* 2002; 288: 321.
20. Torgerson DJ, Bell-Syer SE. Hormone replacement therapy and prevention of nonvertebral fractures: A meta-analysis of randomized trials. *JAMA* 2001; 285: 2891.
21. Michaelsson K, Baron JA, Farahmand BY, et al. Hormone replacement therapy and risk of hip fracture: Population based case control study. The Swedish Hip Fracture Study Group. *BMJ* 1998; 316: 1858.
22. Johnson J, Canning J, Kaneko T, et al. Germline stem cells and follicular renewal in the postnatal mammalian ovary. *Nature* 2004; 428: 145.
23. Johnson J, Bagley J, Skaznik-Wikiel M, et al. Oocyte generation in adult mammalian ovaries by putative germ cells in bone marrow and peripheral blood. *Cell* 2005; 122: 303.
24. Teitelbaum, S.L. Bone resorption by osteoclasts. *Science* 2000; 289: 1504.
25. Kushida T, Inaba M, Hisha H, et al. Crucial role of donorderived stromal cells in successful treatment for intractable autoimmune diseases in MRL/lpr mice by BMT via portal vein. *Stem Cells* 2001; 19: 226.
26. Pereira RF, O'Hara MD, Laptev AV, et al. Marrow stromal cells as a source of progenitor cells for nonhematopoietic tissues in transgenic mice with a phenotype of osteogenesis imperfecta. *Proc Natl Acad Sci USA* 1998; 95: 1142.
27. Makino S, Fukuda K, Miyoshi S, et al. Cardiomyocytes can be generated from marrow stromal cells in vitro. *J Clin Invest* 1999; 103: 697.
28. Woodbury D, Schwarz EJ, Prockop DJ, Black IB. Adult rat and human bone marrow stromal cells differentiate into neurons. *J Neurosci Res* 2000; 61: 364.
29. Okazaki R, Inoue D, Shibata M, et al. Estrogen promotes early osteoblast differentiation and inhibits adipocyte differentiation in mouse bone marrow stromal cell lines that express estrogen receptor (ER)$-\alpha$ or $-\beta$. *Endocrinology* 2002; 143: 2349.
30. Qu Q, Perala-Heape M, Kapanen A, et al. Estrogen enhances differentiation of osteoblasts in mouse bone marrow culture. *Bone* 1998; 22: 201.

31. Lee WY, Cho SW, Oh ES, et al. The effect of bone marrow transplantation on the osteoblastic differentiation of human bone marrow stromal cells. *J Clin Endocrinol Metab* 2002; 87: 329.
32. Wang Z, Goh J, Das De S. Efficacy of bone marrow-derived stem cells in strengthening osteoporotic bone in a rabbit model. *Tissue Eng* 2006; 12: 1753.
33. Ergun H, Howland WJ. Postradiation atrophy of mature bone. *CRC Crit Rev Diagn Imaging* 1980; 12: 225.
34. Hopewell JW. Radiation-therapy effects on bone density. *Med Pediatr Oncol* 2003; 41: 208.
35. Keller PJ, Maurer-Major E. Hormone substitution in menopause. *Schweiz Rundsch Med Prax* 1997; 86: 1458.
36. Ness J, Aronow WS, Beck G. Menopausal symptoms after cessation of hormone replacement therapy. *Maturitas* 2006; 53: 356.
37. Wang X, Chen H, Yin H, et al. Fertility after intact ovary transplantation. *Nature* 2002; 415: 385.

Clinical and Experimental Immunology ORIGINAL ARTICLE doi:10.1111/j.1365-2249.2008.03588.x

The Wistar Bonn Kobori rat, a unique animal model for autoimmune pancreatitis with extrapancreatic exocrinopathy

Y. Sakaguchi,*† M. Inaba,* M. Tsuda,* G. K. Quan,* M. Omae,* Y. Ando,* K. Uchida,† K. Okazaki† and S. Ikehara*

**First Department of Pathology and †Third Department of Internal Medicine, Kansai Medical University, Moriguchi City, Osaka, Japan*

Accepted for publication 4 December 2007

Correspondence: S. Ikehara, First Department of Pathology, Kansai Medical University, 10-15 Fumizono-cho, Moriguchi City, Osaka 570-8506, Japan.
E-mail: ikehara@takii.kmu.ac.jp

Summary

The male Wistar Bonn/Kobori (WBN/Kob) rat is known to be a unique animal model for chronic pancreatitis with widely distributed fibrosis and degeneration of parenchyma because of the infiltration of lymphocytes. In this report, we show that female (but not male) rats develop dacryoadenitis at 3 months of age, and that both male and female WBN/Kob rats develop sialoadenitis, thyroiditis, sclerotic cholangitis and tubulointerstitial nephritis over 18 months of age. The infiltration of $CD8^+$ cells and the deposits of tissue-specific IgG2b were observed in the injured pancreas and lachrymal glands. Furthermore, the number of regulatory T cells (defined as $CD4^+$ Forkhead box $P3^+$ cells) decreased in the periphery of both male and female WBN/Kob rats, suggesting that the onset of these diseases is attributable, at least, to the failure in the maintenance of peripheral immune tolerance. These features show clearly that WBN/Kob rats are a useful animal model for autoimmune pancreatitis and Sjøgren-like syndrome or multi-focal fibrosclerosis in humans. We also show that these autoimmune diseases can be prevented by a newly devised strategy of bone marrow transplantation (BMT) in which bone marrow cells are injected directly into the bone marrow cavity: intrabone marrow–BMT.

Keywords: animal model, autoimmune extrapancreatic exocrinopathy, autoimmune pancreatitis, Forkhead box P3, intra bone marrow–bone marrow transplantation

Introduction

Recently, autoimmune pancreatitis (AIP) has been reported as a part of chronic pancreatitis with pancreatic duct stenosis. AIP is characterized by hypergammaglobulinaemia and responsiveness to corticosteroid therapy, suggesting the involvement of autoimmune mechanisms, particularly at the onset of this disease [1]. Patients with autoimmune diseases such as Sjøgren's syndrome and other autoimmune diseases in the liver, bile ducts, intestine and blood vessels often show AIP [2]. Lesions in the pancreas have been observed in acinar cells, ductal cells and pancreatic islet cells, indicating that the target cells or target molecules for autoimmune reactions are considered to be variable [3]. The precise mechanism underlying the onset of AIP and its progress is still unknown [4], although the diagnosis and therapy have been investigated extensively and progressed. In various cases of pancreatitis, it is difficult to prove whether autoimmune mechanisms are involved in the development of pancreatitis [5]. Therefore, long-term studies on histopathological evaluation before the onset of pancreatitis are clinically important [6]. Imaging studies of patients with AIP characteristically show the diffuse enlargement of the pancreas and irregular narrowing of the main pancreatic duct. Typical immunological abnormalities are the elevation of serum IgG4 and the presence of autoantibodies. The histopathological findings show lymphoplasmacytic sclerosing pancreatitis (LPSP) associated with fibrotic changes with dense infiltration of lymphocytes and IgG4-positive plasma cells [7]. However, the role of IgG4 in the pathogenesis of AIP still remains unclear. Therefore, the establishment of an animal model for AIP is critically important. To date, there have been reported various artificial AIP models, most of which are chemical or antigen-induced ones [8,9]. Even if there are some spontaneous animal models which partially resemble human AIP [10,11], there are many differences in terms of symptoms, gene functions and pathological findings.

It has been shown that the male Wistar Bonn/Kobori (WBN/Kob) rat is an animal model for spontaneous diabetes, osteopenia and systemic haemosiderin deposition

[12]. Spontaneous hyperglycaemia, glycosuria, hypoinsulinaemia and glucose intolerance are observed after the age of 17 months. Marked fibrosis is observed around the pancreatic ducts and blood vessels at 3–6 months of age [13,14]. The fibrous tissue gradually invades extensive areas of the pancreas, and the islets are also affected by fibrotic degeneration, leading to an obvious decrease in islet number and size. Distinct infiltration of inflammatory cells has been observed around the islets and among adjacent acinar cells, and most inflammatory cells are apparently lymphocytes. Macrophages or granulocytes are not often observed in the lesions. These pathological findings are found in male but not female WBN/Kob rats, and have been discussed regarding their pathogenesis in relation to sex hormone [15], genetic factor [16] and immune disturbance [17]. WBN/Kob rats have some interesting characteristics: (i) only male WBN/Kob rats appear with pancreatitis; (ii) they are a unique diabetic animal model whose islets are withered by progress with inflammatory fibrosis dissimilar to the other diabetic models [18,19]; (iii) infiltrating cells are nearly all lymphocytes, rather than plasma cells and eosinophils [12]; and (iv) immune suppressive drugs such as tacrolimus or steroid hormones could prevent the onset of pancreatitis [17]. These characteristics resemble human AIP.

We have shown previously that conventional allogeneic bone marrow transplantation (BMT) can be used to treat autoimmune disease using various autoimmune-prone mice [20,21]. Recently, we have developed a new BMT method in which donor bone marrow cells (BMCs) are injected directly into the bone marrow cavity of recipients: intrabone marrow–BMT (IBM–BMT) [22,23]. This strategy allows us to reduce radiation doses to 5 Gy × 2 (fractionated irradiation), which is equivalent to 8 Gy (one shot). Therefore, we attempted to prevent abnormal pathological, serological and immunological findings in the WBN/Kob rats by IBM–BMT; in our preliminary experiments, conventional BMT was found to be unable to be used to prevent these abnormalities in the rats. In line with these studies, the model described here can be considered to be highly relevant not only for a better understanding of the pathogenesis of AIP but also for the preclinical testing of novel strategies for the treatment of AIP.

Materials and methods

Rats

Male and female WBN/Kob rats (RT1a^u), male Wistar rats and Fischer 344 (F344:RT1a^l) rats were purchased from SLC (Shizuoka, Japan). They were maintained until use in our animal facilities under specific pathogen-free conditions. All experimental protocols were approved by the Animal Experimentation Committee (06-026), Kansai Medical University.

Histopathological analysis

Histopathological studies of the systemic exocrine organs (pancreas, liver, lachrymal and parotid glands, kidney and thyroid) in male and female WBN/Kob rats 4 weeks, 12 weeks and 18 months of age were performed. In brief, each organ was fixed in paraformaldehyde and infiltrated with Histo-Clear (National Diagnostics, Atlanta, GA, USA) [24]. They were dehydrated with ethanol and embedded in paraffin (5 μm), and stained with haematoxylin and eosin or Masson-Trichrome and Sirius red to detect fibrosis.

Immunohistochemical analyses

Thyroid, liver and kidney from 18-month-old WBN/Kob rats, and pancreas, spleen, lachrymal gland and parotid gland were obtained serially from the recipients 4, 8, 12 and 16 weeks after IBM–BMT. The sections were prepared with the masked antigen for using Histo-Clear, rehydrated through a graded series of ethanol/water solutions and incubated at 85°C in antigen retrieval buffer. The specimens were also stained with fluorescein isothiocyanate (FITC)-, phycoerythrin (PE)- or biotin-conjugated IgG, IgG1, IgG2a, IgG2b and IgG2c (FITC–streptavidin was used to visualize biotin-conjugated antibodies). Nuclei were stained with 4,6-diamidino-2-phenylindole (Nacalai Tesque, Inc., Kyoto, Japan). Immunohistochemical staining for $CD4^+$, $CD8^+$ cells, anti-major histocompatibility complex (MHC) I (OX-18) and anti-MHC II (OX-6) were also performed using frozen tissues from pancreas and lachrymal gland. The sections (4 μm) were incubated with appropriate primary antibodies at 4°C overnight. They were incubated with biotinylated secondary anti-rat IgG antibodies (Vector Laboratories, Burlingame, CA, USA) and incubated with avidin–biotin horseradish peroxidase complex (Vector Laboratories). Samples were incubated with 3,3′-diaminobenzidine in the presence of H_2O_2 to develop the chromatic reaction. The stained samples were analysed using an optical microscope (Nikon Eclipse E1000M, Digital Sight ACT-1 for L-1 software version 2·62; Nikon Co. Ltd, Tokyo, Japan) and confocal laser microscope (LSM 510 META; Carl Zeiss IMT Corporation, Oberkochen, Germany).

Biochemical analyses

Blood glucose was measured by a Dextor ZIIR (Bayer Medical Ltd, Tokyo, Japan). Total amylase and total protein were determined by a biochemistry automated analyser (AU5400; Olympus Corp., Tokyo, Japan). Immunoelectrophoresis was carried out in our laboratory using standard equipment. Interleukin (IL)-4, IL-10 and IL-12 were analysed by an enzyme-linked immunosorbent assay kit (R&D Systems, Inc., Minneapolis, MN, USA; BioSource, Camarillo, CA, USA).

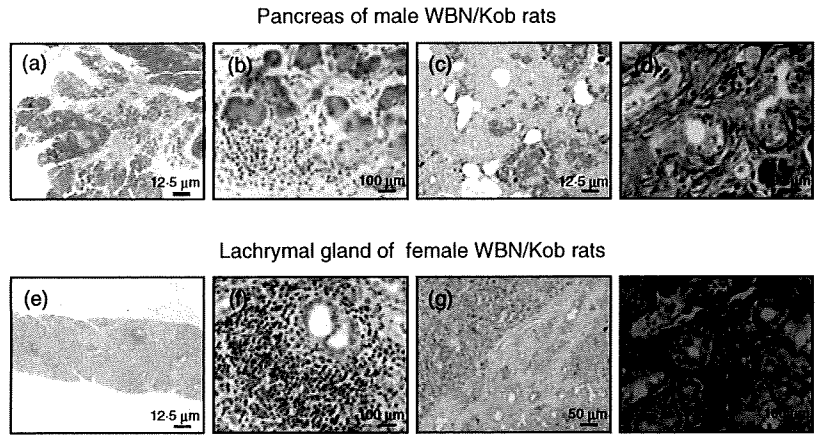

Fig. 1. Pathological findings of pancreas and lachrymal grand of male and female Wistar Bonn/Kobori (WBN/Kob) rats. Paraffin sections of pancreas and lachrymal gland were prepared and stained with haematoxylin and eosin (H&E) (6 months of age). (a,b,e,f) Stained with H&E, (c) and (g); stained with Masson-Trichrome, (d) and (h); stained with Sirius red. Bars in the figure represent scales.

IBM–BMT experiments

Fludarabine at 50 mg/kg was given as a single intravenous injection and irradiated in fractionated irradiations (5·0 Gy × 2 = 10 Gy; 4-h interval) 1 day before transplantation. BMCs were collected from the femurs and tibias of Fischer 344 rats. $CD4^+$ cells were depleted from the BMCs by the combination of anti-CD4 antibody (Caltag Laboratories, Burlingame, CA, USA) and sheep anti-mouse IgG-coupled Dynabeads® (Dynal, Oslo, Norway). Resultant $CD4^+$ T cell-depleted BMCs (2×10^8 BMCs) were injected directly into the bone marrow cavity of the recipient's tibia (IBM–BMT) to facilitate the early recovery of haematopoiesis and donor cell engraftment [22]. In brief, the region from the thigh to the knee joint was shaved of hair with a razor. The knee was flexed to 90°, and the proximal side of the tibia was drawn to the anterior. A 21-gauge needle was inserted into the joint surface of the tibia through the patellar tendon and then inserted into the bone marrow cavity. Using a microsyringe (50 μl; Hamilton Co., Reno, NV, USA), the donor BMCs (3×10^7/30 μl) were injected into the bone marrow cavity. These WBN/Kob rats are abbreviated as (F344→WBN/Kob).

Surface marker analyses

The spleen cells, peripheral blood mononuclear cells or BMCs were prepared from recipient rats, and the cells were then stained with FITC-anti-$RT1A^l$ monoclonal antibodies (mAb) (PharMingen, San Diego, CA, USA) to identify the donor-derived cells. Donor-derived cells bearing a lineage-specific phenotype were also analysed by FITC-anti-$RT1A^l$ mAb plus PE-conjugated mAb against CD45R (B220) (PharMingen), CD4, CD8 or CD11b (Caltag Laboratories). Furthermore, the cells were stained with anti-CD4 and anti-CD25 mAb (BD Pharmingen, Hamburg, Germany) or anti-CD4 and anti-Forkhead box P3 (FoxP3) mAb to detect regulatory T cells (T_{regs}). In the case of staining with anti-FoxP3 mAb, cells were stained with FITC-anti-CD4 mAb, and then fixed and permeabilized with Cutofix/Cytoperm solution™ (BD Pharmingen). The cells thus treated were stained intracytoplasmically with PE-anti-FoxP3 mAb (eBioscience, Inc., San Diego, CA, USA). The stained cells were analysed by a fluorescence activated cell sorter (FACScan®; Becton Dickinson, Mountain View, CA, USA).

Statistical analysis

Survival data were analysed using the Kaplan–Meier method using StatMate software. Differences between groups were analysed using the log-rank test in the StatMate software. $P < 0.05$ was considered to be significant.

Results

Histopathological and immunological features of WBN/Kob rats

After 4 weeks of age male WBN/Kob rats showed chronic pancreatitis, while after 4 weeks of age female WBN/Kob rats showed Sjøgren-like dacryoadenitis. Histopathologically, significant oedema in the interstitium, the infiltration of lymphocytes and the destruction of acinar cells were seen in the pancreas of male WBN/Kob rats (Fig. 1a and b). At approximately 8 weeks of age fibrosis appeared in the lobules, and after 12 weeks of age the infiltration of inflammatory cells, oedema, haemorrhage and the deposit of haemosiderin were found in the interlobules or peri-pancreatic ducts, leading to the isolation of acini and pancreatic islets, followed by acceleration of fibrosis (Fig. 1c and d). On the other hand, in female WBN/Kob rats, the infiltration of inflammatory cells was found in the outer lachrymal glands after the age of 4 weeks, and the inflammation was aggravated dually. Significant infiltration of lymphocytes was noted in the periductal area, and the acceleration of fibrosis was found in the interlobules (Fig. 1g and h), although the lobular structure in the outer lachrymal glands was still maintained (Fig. 1e and f). Furthermore, many vacuoles and the degeneration

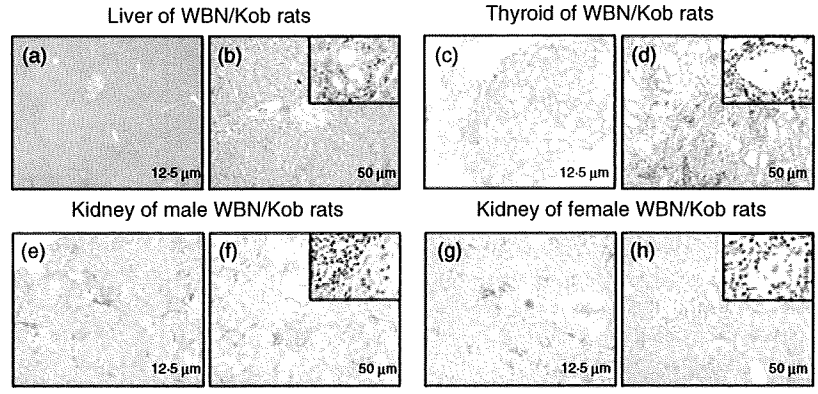

Fig. 2. Pathological findings of liver, thyroid and kidney in the aged Wistar Bonn/Kobori (WBN/Kob) rats. Twenty months after birth, liver, thyroid and kidney were removed and paraffin sections were stained with haematoxylin and eosin. (a, b) Liver; (c,d) thyroid; (e,f) kidney of male WBN/Kob rat; (g,h) kidney of female WBN/Kob rat.

of nucleus structure were detected in acinar cells. Thus, chronic dacryoadenitis (and partially parotiditis) resembling Sjøgren's syndrome was found in female WBN/Kob rats.

In aged male and female WBN/Kob rats (>18 months of age), sclerotic cholangitis, thyroiditis and even tubulointerstitial nephritis were observed along with pancreatitis and dacryoadenitis. The infiltration of inflammatory cells was found in the area of peripheral bile ducts, and hyperplasia of bile ducts and the fibrosis of peri-bile duct areas were also observed (Fig. 2a and b), resembling sclerotic cholangitis in humans. Colloids in the thyroid glands were found to be degenerated and partially destroyed. Infiltration of the inflammatory cells was detected in hyperplastic and fibrous interstitium (Fig. 2c and d). Furthermore, in male WBN/Kob rats, the hyperplasia of the mesangial cells and the demilune bodies in the uriniferous tubule were found clearly as evidence of diabetic nephritis associated with tubulointerstitial nephritis. Infiltration of the inflammatory cells was also detected in the interstitium as tubulointerstitial nephritis (Fig. 2e and f). On the other hand, infiltration of the inflammatory cells was detected only in the interstitium in female WBN/Kob rats where pancreatitis was not developed (Fig. 2g and h). Thus, it is noted that there are clear sex differences in pathological findings.

Immunohistochemical analyses revealed that a large number of $CD8^+$ T cells were observed in the injured organs (Fig. 3b pancreas; Fig. 3f lachrymal gland), while a small number of $CD4^+$ T cells were infiltrated into the pancreas (Fig. 3a) and lachrymal gland (Fig. 3e). The expression of both MHC class II (Fig. 3c pancreas; Fig. 3g lachrymal gland) and MHC class I (Fig. 3d pancreas; Fig. 3h lachrymal gland) was also found, although the former was less than the latter.

Serum γ-globulin levels increased in both male and female WBN/Kob rats (Fig. 4), and the deposits of γ-globulin were also observed in the pancreas of male WBN/Kob rats and in the lachrymal gland of female rats. IgG, which was detected specifically in the injured region, was IgG2b subclass, but not any other subclass (Fig. 5) (IgG2c appeared with non-specific staining), and IgG2b was actually detected in the B cells which appeared in the injured region (Fig. 6i and j pancreas; Fig. 6l and m lachrymal gland) along with $CD8^+$ T cells (Fig. 6c pancreas; Fig. 6h lachrymal gland). These findings indicate clearly that pancreatitis in male WBN/Kob rats and dacryoadenitis in female WBN/Kob rats develop as a result of immunological disorders, and can be categorized as AIP and autoimmune dacryoadenitis.

The involvement of immunological disorders in the onset of pancreatitis and dacryoadenitis was confirmed by the measurement of T_{regs} known to control negatively autoreactive T cells in the periphery. When compared with normal controls (F344), the number of T_{regs} (detected as $CD4^+$ $FoxP3^+$ cells in the spleen cells) was decreased significantly in WBN/Kob rats (~7% in WBN/Kob rats at 8 weeks, ~10% in

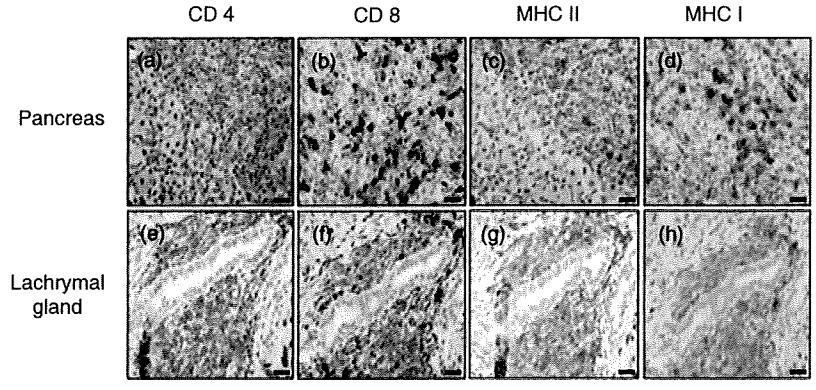

Fig. 3. Immunohistological staining for $CD4^+$, $CD8^+$, major histocompatibility complex (MHC) I and anti-MHC II T cells. Pancreas and lachrymal gland were removed (4 months of age) and serial sections were stained with anti-CD4, anti-CD8 anti-MHC I and anti-MHC II monoclonal antibody. (a–d) Pancreas of male Wistar Bonn/Kobori (WBN/Kob) rat; (e–h) pancreas of female WBN/Kob rat.

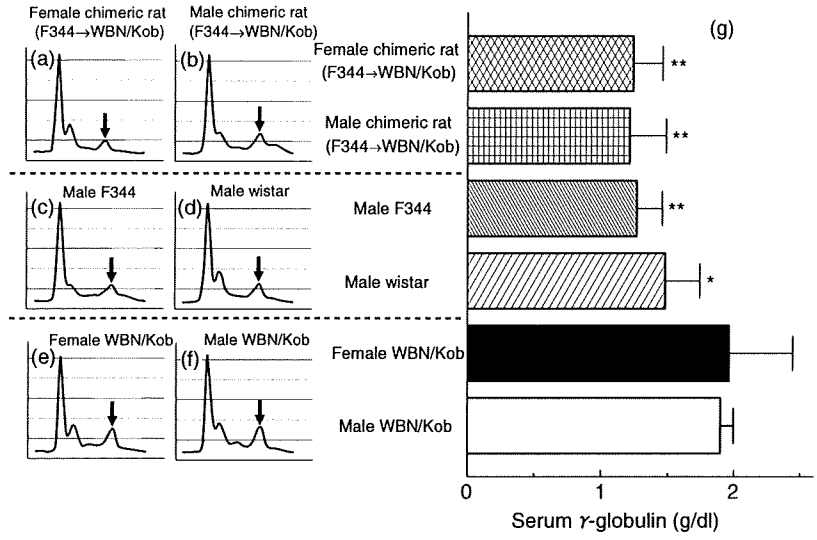

Fig. 4. Analyses of serum γ-globulin. Sera were collected from male and female Wistar Bonn/Kobori (WBN/Kob) rat (4 months of age) and electrophoresis was carried out to examine the relative level of IgG. (a) Female WBN/Kob rat treated with intrabone marrow–bone marrow transplantation (IBM–BMT) from F344 (F344→Kob); (b) male WBN/Kob rat treated with IBM–BMT from F344 (F344→WBN/Kob); (c) male F344 rat as a normal control; (d) male Wistar rat as a normal control; (e) untreated female WBN/Kob rat; (f) untreated male WBN/Kob rat; and (g) amounts of γ-globulin in sera calculated from the results of electrophoresis and total amounts of serum protein. Columns and bars represent means ± standard deviations of seven rats. $^*P < 0.05$; $^{**}<0.01$.

untreated normal F344 rats). The frequency of T_{regs} decreased gradually to ~4% in male WBN/Kob rats and to ~6% in females at 20 weeks (Fig. 7f), and the representative fluorescence activated cell sorter profiles are shown in Fig. 6a–e.

Effects of IBM–BMT on the development of pancreatitis and dacryoadenitis

We have found recently that IBM–BMT can facilitate the engraftment of not only donor-derived haemopoietic cells but also mesenchymal stem cells (bone marrow stromal cells), and thereby prevent or treat various intractable diseases [22,25,26]. We therefore applied this strategy to the prevention of pancreatitis and dacryoadenitis in WBN/Kob rats.

We first examined chimerism in the WBN/Kob rats that had received BMCs of donor F344 rats by IBM–BMT [(F344→WBN/Kob)]. Chimerism was analysed flow cytometrically using FITC-conjugated donor-specific anti-RT1A^1 mAb. As shown in Fig. 7 [compare (a, b, c) with (d,e)], haematolymphoid cells were of donor origin and the donor chimerism remained stable until the experiments were finished (20 weeks of age). The tolerant state was confirmed by mixed lymphocyte reaction. Splenic T cells from (F344→WBN/Kob) rats were used as responders and stimulated with irradiated spleen cells from F344 and unrelated BN rats. T cells from (F344→Kob) rats responded significantly to the unrelated BN spleen cells, but not to the spleen cells of F344 or WBN/Kob rats (data not shown), indicating that the T cells of (F344→WBN/Kob) rats were tolerant of the donor and recipient MHCs, but could respond to the third-party MHC determinants.

After IBM–BMT, the male or female recipients [(F344→WBN/Kob)] did not develop pancreatitis (Fig. 8b and c) or dacryoadenitis (Fig. 8g and h) respectively, showing no hyperglycaemia for more than 16 months (Fig. 9b) after IBM–BMT in the male recipients [(F344→WBN/Kob)], whereas chronic pancreatitis (Fig. 8d and e) or dacryoadenitis (Fig. 8i and j) was observed in the untreated WBN/Kob rats with the destruction of pancreatic islets, and hyperglycaemia was observed at 1 month and thereafter elevated gradually more than 400 mg/dl at 20 weeks of age. Infiltration of $CD8^+$ and $CD4^+$ T cells in the pancreas or lachrymal glands was not detected in the recipients [(F344→WBN/Kob)] (data not shown), and the frequency of T_{regs} in the periphery and spleen was normalized in both male and female (F344→WBN/Kob) rats and maintained even 20 weeks after IBM–BMT (Fig. 7f).

In accordance with the amelioration of pancreatitis or dacryoadenitis, serum amylase (Fig. 9a) and γ-globulin levels (Fig. 4) were normalized, and hyperglycaemia observed in the untreated male WBN/Kob rats was not detected (Fig. 9b).

Measurement of cytokines

To analyse the mechanism underlying the development of AIP and dacryoadenitis in the WBN/Kob rats, we next examined kinetically the cytokine levels of untreated WBN/Kob rats. The production of IL-10 in male and female WBN/Kob rats decreased at 3 months of age and remained unchanged to 20 months (Fig. 9f). In contrast, serum IL-12 levels in WBN/Kob rats increased at the age of 3 months, and the elevated levels of IL-12 were maintained until 20 months (Fig. 9d). The levels of IL-4 were slightly higher in male and female WBN/Kob rats than in the control male F344 rats, but there was statistically no significant difference between them (Fig. 9e).

Discussion

This study was carried out to clarify whether autoimmune mechanisms are involved in the development of pancreatitis

